



OPEN ACCESS

Original research

# TREM-2 defends the liver against hepatocellular carcinoma through multifactorial protective mechanisms

Aitor Esparza-Baquer,<sup>1</sup> Ibone Labiano,<sup>1</sup> Omar Sharif,<sup>2,3</sup> Aloña Agirre-Lizaso,<sup>1</sup> Fiona Oakley,<sup>4</sup> Pedro M Rodrigues,<sup>1,5</sup> Ekaterina Zhuravleva,<sup>6</sup> Colm J O'Rourke,<sup>6</sup> Elizabeth Hijona,<sup>1,5</sup> Raul Jimenez-Agüero,<sup>1</sup> Ioana Riaño,<sup>1</sup> Ana Landa,<sup>1</sup> Adelaida La Casta,<sup>1</sup> Marco Y W Zaki ,<sup>4,7</sup> Patricia Munoz-Garrido,<sup>6</sup> Mikel Azkargorta,<sup>5,8</sup> Felix Elortza,<sup>5,8</sup> Andrea Vogel ,<sup>2,3</sup> Gernot Schabbauer,<sup>2,3</sup> Patricia Aspichueta,<sup>9</sup> Jesper B Andersen ,<sup>6</sup> Sylvia Knapp,<sup>10,11</sup> Derek A Mann,<sup>4</sup> Luis Bujanda,<sup>1,5,12</sup> Jesus Maria Banales ,<sup>1,5,13</sup> Maria Jesus Perugorria <sup>1,5,12,13</sup>

► Additional material is published online only. To view please visit the journal online (<http://dx.doi.org/10.1136/gutjnl-2019-319227>).

For numbered affiliations see end of article.

## Correspondence to

Maria Jesus Perugorria and Jesus Maria Banales, Department of Liver and Gastrointestinal Diseases, Biodonostia Health Research Institute, Donostia University Hospital, Donostia - San Sebastián, Guipuzcoa, Spain; [matxus.perugorria@biodonostia.org](mailto:matxus.perugorria@biodonostia.org); [jesus.banales@biodonostia.org](mailto:jesus.banales@biodonostia.org)

AE-B and IL are joint first authors.

JMB and MJP are joint senior authors.

Received 4 June 2019  
Revised 20 July 2020  
Accepted 23 July 2020  
Published Online First  
9 September 2020



► <http://dx.doi.org/10.1136/gutjnl-2020-322638>



© Author(s) (or their employer(s)) 2021. Re-use permitted under CC BY-NC. No commercial re-use. See rights and permissions. Published by BMJ.

**To cite:** Esparza-Baquer A, Labiano I, Sharif O, *et al.* Gut 2021;**70**:1345–1361.

## ABSTRACT

**Objective** Hepatocellular carcinoma (HCC) is a prevalent and aggressive cancer usually arising on a background of chronic liver injury involving inflammatory and hepatic regenerative processes. The triggering receptor expressed on myeloid cells 2 (TREM-2) is predominantly expressed in hepatic non-parenchymal cells and inhibits Toll-like receptor signalling, protecting the liver from various hepatotoxic injuries, yet its role in liver cancer is poorly defined. Here, we investigated the impact of TREM-2 on liver regeneration and hepatocarcinogenesis.

**Design** TREM-2 expression was analysed in liver tissues of two independent cohorts of patients with HCC and compared with control liver samples. Experimental HCC and liver regeneration models in wild type and *Trem-2*<sup>-/-</sup> mice, and *in vitro* studies with hepatic stellate cells (HSCs) and HCC spheroids were conducted.

**Results** TREM-2 expression was upregulated in human HCC tissue, in mouse models of liver regeneration and HCC. *Trem-2*<sup>-/-</sup> mice developed more liver tumours irrespective of size after diethylnitrosamine (DEN) administration, displayed exacerbated liver damage, inflammation, oxidative stress and hepatocyte proliferation. Administering an antioxidant diet blocked DEN-induced hepatocarcinogenesis in both genotypes. Similarly, *Trem-2*<sup>-/-</sup> animals developed more and larger tumours in fibrosis-associated HCC models. *Trem-2*<sup>-/-</sup> livers showed increased hepatocyte proliferation and inflammation after partial hepatectomy. Conditioned media from human HSCs overexpressing TREM-2 inhibited human HCC spheroid growth *in vitro* through attenuated Wnt ligand secretion.

**Conclusion** TREM-2 plays a protective role in hepatocarcinogenesis via different pleiotropic effects, suggesting that TREM-2 agonism should be investigated as it might beneficially impact HCC pathogenesis in a multifactorial manner.

## INTRODUCTION

Hepatocellular carcinoma (HCC) is the sixth most common cancer and the third leading cause of cancer-related mortality worldwide. HCC usually

## Significance of this study

### What is already known on this subject?

- Hepatocellular carcinoma (HCC) is a prevalent cancer and its pathogenesis is a multistep process involving the progressive accumulation of molecular alterations. HCC usually arises on a background of chronic liver injury involving inflammatory and hepatic regenerative processes.
- Increasing evidence suggests the gut–liver axis and innate immunity play a critical role in the development and progression of several liver diseases, including HCC. Fine-tuning of Toll-like receptor (TLR)-driven inflammation during liver cancer is key.
- The triggering receptor expressed on myeloid cells 2 (TREM-2) negatively regulates TLR-mediated inflammatory responses.
- TREM-2 is expressed on non-parenchymal liver cells and is upregulated during diverse forms of liver injury in humans and mice. TREM-2 promotes the resolution of inflammation during diverse types of hepatic injury, ultimately preventing parenchymal cell death.

arises on the background of chronic liver injury and inflammation, mainly triggered by infectious agents (eg, hepatitis B and C virus), alcohol abuse and/or excessive hepatocellular fat accumulation.<sup>1</sup> During the past few years, it has become evident that innate immunity plays a critical role in the development and progression of several liver diseases, including HCC.<sup>2</sup>

The triggering receptor expressed on myeloid cells 2 (TREM-2) is an anti-inflammatory receptor that negatively regulates toll-like receptor (TLR)-mediated inflammatory responses, whereas the proinflammatory receptor TREM-1 augments TLR-induced inflammation.<sup>3 4</sup> Both receptors signal through the immunoreceptor tyrosine-based

## Significance of this study

## What are the new findings?

- ▶ TREM-2 expression is upregulated in human HCC tissue, in mouse models of liver regeneration and HCC.
- ▶ In human HCC tumours, TREM-2 is expressed in infiltrating monocyte derived macrophages.
- ▶ *Trem-2*<sup>-/-</sup> mice developed increased number of liver tumours after diethylnitrosamine (DEN) administration, displayed exacerbated liver damage, inflammation, oxidative stress and hepatocyte proliferation.
- ▶ Liver cancer in *Trem-2*<sup>-/-</sup> mice is associated with elevated reactive oxygen species levels and the administration of an antioxidant diet blocked DEN-induced DNA damage and hepatocarcinogenesis in these animals.
- ▶ In fibrosis-associated HCC models, *Trem-2*<sup>-/-</sup> mice also exhibited elevated tumour burden and less fibrosis.
- ▶ *Trem-2*<sup>-/-</sup> livers exhibited increased hepatocyte proliferation and inflammation after partial hepatectomy (PHx). The suppressive effects of this receptor on hepatocyte proliferation were linked to its effects on early inflammatory events post-PHx.
- ▶ In line with TREM-2 effects on inflammation and proliferation, conditioned media from human hepatic stellate cells overexpressing TREM-2 inhibited human HCC spheroid growth *in vitro*.

## How might it impact on clinical practice in the foreseeable future?

- ▶ While strategies aiming to activate TREM-2 in the context of HCC are warranted, as TREM-2 agonism might beneficially impact tumour burden in a pleiotropic manner, they will require a detailed evaluation for potential profibrotic side-effects.

activation motif of the adaptor protein DAP-12.<sup>5</sup> The ligand(s) for TREM-2 are unknown although numerous are proposed, ranging from various anionic molecules; phospholipids, proteoglycans to apolipoproteins and heat shock proteins.<sup>6–9</sup> TREM-2 has been mainly studied in the brain, where its deficiency in microglia is associated with several neurodegenerative disorders, including Alzheimer's disease.<sup>10–12</sup> The role of TREM-2 in cancer is poorly understood, although several studies suggest that high TREM-2 expression correlates with worsened outcome during various cancers including gastric, glioma and renal cell carcinoma.<sup>13–15</sup> On the other hand, in the liver, we recently described that TREM-2 is predominantly expressed in non-parenchymal cells (ie, Kupffer cells (KCs) and hepatic stellate cells (HSCs)), where it serves to attenuate TLR4-mediated cytokine production.<sup>16</sup> Notably, herein we could show that mice deficient for *Trem-2* displayed increased liver damage and inflammation post-acetaminophen and acute or chronic carbon tetrachloride (CCl<sub>4</sub>) administration. Given the crucial role of innate immunity in HCC, we hypothesised that TREM-2 could play a protective role in its development and progression.

## MATERIALS AND METHODS

## Patients

TREM-2 expression was determined in 366 HCC and 49 non-tumour tissues surrounding HCC from the RNAseq data of the cancer genome atlas (TCGA) ('TCGA cohort') in Reads per Kilobase Million. Level 3 RNA-seq data generated by The Cancer Genome Atlas Liver Hepatocellular Carcinoma

(TCGA-LIHC) consortium were downloaded from the National Cancer Institute Genomic Data Commons (<https://gdc.cancer.gov/>).<sup>17</sup> Moreover, 35 HCC human biopsies of different etiologies and 21 control liver tissues (from non-neoplastic liver tissue of patients with colorectal hepatic metastasis) were obtained from the Biobank of Donostia University Hospital ('San Sebastian cohort') for the analysis of TREM-2 expression and several pro-fibrotic and pro-inflammatory genes by quantitative polymerase chain reaction (qPCR). Patient information is detailed in online supplementary table 1. Samples and clinicopathological information were obtained from the Basque Biobank. Single-cell transcriptome profiling of human HCC tumour biospecimens from nine HCC tumours was downloaded from Gene Expression Omnibus (GSE125449). Patient specific characteristics of this data set are previously described and all patients provided informed consent.<sup>18</sup> Briefly, HCC tumour samples of various aetiologies were obtained by resection or needle biopsy from five males (ages 61–77) and four females (ages 41–64), with several patients receiving immunotherapy.<sup>18</sup>

## Animal models

*Wild type* (WT) C57BL/6 and *Trem-2*<sup>-/-</sup> mice backcrossed onto a >98% C57BL/6 background were generated as previously described.<sup>3</sup> Mice were bred and housed at the animal facility of the Biodonostia Health Research Institute in the same room under specific pathogen free conditions with microisolator tops. All experiments were performed under approval of the Animal Experimentation Ethics Committee of the Institution.

HCC was induced in WT and *Trem-2*<sup>-/-</sup> male mice by the administration of a single intraperitoneal injection of the hepatocarcinogen diethylnitrosamine (DEN; Sigma-Aldrich) (30 mg/kg of DEN dissolved in 0.9% saline) at 15 days of age. Mice were humanely killed at 30 or 40 weeks post-injection. To evaluate the role of reactive oxygen species (ROS), 15 weeks after DEN administration, both genotypes were fed a diet supplemented with 0.7% w/w of the antioxidant butylated hydroxyanisole (BHA; Sigma-Aldrich) for another 15 weeks prior to sacrifice. To evaluate effects of acute DEN treatment on the liver, 8 week-old male WT and *Trem-2*<sup>-/-</sup> mice were injected with 100 mg/kg DEN and sacrificed 6, 24 and 72 hours post-injection. Regenerative responses were evaluated in 8 week-old male WT and *Trem-2*<sup>-/-</sup> mice using partial hepatectomy (PHx ~70%), as previously described.<sup>19</sup> To stain proliferating hepatocytes, mice were intraperitoneally injected with 150 mg/kg of 5'-bromo-2'-deoxyuridine (BRDU; Sigma-Aldrich) 2 hours before humane killing. Fibrosis-associated HCC was induced in WT and *Trem-2*<sup>-/-</sup> male mice by combining chronic DEN administration (30 mg/kg, intraperitoneal, 15 days post-partum) with 10 weekly injections (one injection per week) of CCl<sub>4</sub> at 2 μL/g body weight (CCl<sub>4</sub>/olive oil 1:3 (vol:vol)), starting at 4 weeks of age (2 weeks after DEN injection). Mice were humanely killed 30 weeks after DEN injection. As a second approach for fibrosis-associated HCC, 8 week-old WT and *Trem-2*<sup>-/-</sup> male mice were administered 0.03% (w/v) thioacetamide (TAA) (Sigma-Aldrich) in drinking water for 40 weeks. Tumour volume in animals was calculated using the formula  $Tv = (W(2) \times L)/2$ .<sup>20</sup>

Gain-of-function experiments were performed overexpressing TREM-2 in 8-week-old WT C57BL/6 mice by intravenous tail vein injection with control (AAV8-CMV-eGFP; VECTOR Biosystems) or *Trem-2* overexpressing adeno-associated viruses (AAV8-CMV-TREM-2-IRES-eGFP; VECTOR Biosystems) ( $1 \times 10^{11}$  pfu) dissolved in 0.9% saline. Next, 72 hours after AAV

injection, mice were injected with DEN (100 mg/kg) and sacrificed 72 hours post-DEN.

### Statistical analysis

Statistical analysis was performed with GraphPad Prism V.6.00 software (GraphPad Software, San Diego, CA). Data are expressed as mean  $\pm$  standard error of the mean (SEM). For comparisons between two groups, parametric Student's *t*-test or non-parametric Mann-Whitney test were used. When more than two groups were compared, one-way analysis of variance with Tukey's posthoc test or Kruskal-Wallis test followed by Dunn's multiple comparison test were used. For correlation analysis, non-parametric Spearman's correlation test was used. Statistically significant differences are represented in figures as \*, \*\*, \*\*\*, \*\*\*\* for *p* values <0.05, <0.01, < 0.001 and <0.0001, respectively.

Additional methods are described in the online supplementary materials.

## RESULTS

### ***TREM-2* is upregulated in human HCC, is prominently expressed in tumour infiltrating macrophages, correlating with markers of inflammation and fibrosis**

To explore a potential role for *TREM-2* in HCC, we first analysed *TREM-2* expression in human HCC tumours and control liver tissue (ie, non-tumour surrounding and healthy liver tissues) using two different approaches (ie, RNA-seq and qPCR) and two different patient cohorts (ie, TCGA and San Sebastian, respectively). Consistent with observations in other cancers including gastric, renal and brain cancers, where elevated *TREM-2* was observed in tumour *versus* control tissues,<sup>13–15</sup> *TREM-2* expression was upregulated in HCC samples compared with non-tumour surrounding liver tissues of the 'TCGA cohort' (figure 1A). Similarly, opposed to normal liver tissues, *TREM-2* levels were increased in HCC tumour tissues of the 'San Sebastian cohort' (figure 1A). Tumour stage stratification of the TCGA cohort revealed that *TREM-2* expression was increased in advanced (T4 stage) *versus* early (T1 stage) HCC tumours (online supplementary figure 1). Evaluating *TREM-2* expression using immunohistochemistry in human healthy liver and HCC tumours of variable aetiology and surrounding cirrhotic liver tissue (online supplementary table 2) verified that *TREM-2* expression was more extensive in diseased compared with control liver (figure 1B). Importantly, while *TREM-2* was not expressed in transformed hepatocytes, *TREM-2* immunostaining was observed in inflammatory periportal areas in the surrounding cirrhotic tissue and adjacent tissue to the fibrotic septa of patients with HCC. Expression was also prominent within infiltrating or resident cells within HCC tumours of various aetiologies and these cells morphologically resembled macrophages (figure 1B and online supplementary figure 2A). We noted that although compared with control liver, *TREM-2* immunostaining was extensive in both the surrounding cirrhotic and tumour tissue of HCC patients in the 'San Sebastian cohort', there was no striking differences in immunostaining intensity between the tumour and its surroundings (figure 1B and online supplementary figure 2A). *TREM-2* mRNA levels (qPCR) of patient matched surrounding *versus* tumour tissue in the 'San Sebastian cohort' demonstrated patient-specific variability with some patients exhibiting down-regulation of *TREM-2* in tumour *versus* surrounding cirrhotic tissue and others upregulation (online supplementary figure 2B). As liver inflammation and fibrosis are important for HCC progression,<sup>1</sup> we next correlated *TREM-2* expression with several

pro-fibrotic (*COL1A1* and *ACTA2*) and pro-inflammatory (*IL1B*, *IL6*, *IL8* and *TNF*) genes in the HCC tumour samples from the 'San Sebastian cohort'. While no correlation was observed for *ACTA2*, *TREM-2* expression positively correlated with *COL1A1*, *IL1B*, *IL6*, *IL8* and *TNF* levels (online supplementary figure 3). Similar results were observed in HCC samples from the TCGA cohort, although *TREM-2* expression here also significantly correlated with *ACTA2* (online supplementary table 3). Thus, compared with control human liver, *TREM-2* expression is increased in HCC tumours and correlates with inflammatory and fibrotic genes.

We next examined which cell types express *TREM-2* in HCC human liver tumours. We utilised publicly available single-cell RNA sequencing data from nine HCC livers, encompassing both malignant and non-malignant cell types<sup>18</sup> and post-data processing, visualised the clustered data using t-distributed Stochastic Neighbour Embedding (t-SNE) through the Seurat R package. In line with previously published observations encompassing this data set,<sup>18</sup> we identified six clusters annotated to T cells, B cells, cancer-associated fibroblasts, tumour-associated macrophages, tumour-associated endothelial cells and hepatic progenitor like (HPC-like) cells using known cell lineage-specific marker genes (figure 1C, online supplementary figure 4). HCC malignant cells were cell annotated based on RNA-seq derived large-scale chromosomal copy-number variations prediction from the previously published work encompassing this data set.<sup>18</sup> These cell types clustered together with HPC-like cells (figure 1C). Notably, this cluster was rich in expression of markers typical of transformed hepatocytes possessing stem/progenitor properties including *alpha-fetoprotein* (*AFP*), *albumin* (*ALB*), *keratin 19* (*KRT19*), *CD24* and *SOX9* (online supplementary figure 5).<sup>21–24</sup> Importantly, and in accordance with our immunohistochemistry data (figure 1B), *TREM-2* expression was most prominent in macrophages and markedly increased compared with malignant cells/transformed hepatocytes (figure 1D,E). Refined-clustering of the macrophage cluster in human HCC, demonstrated distinct clusters with prominent *TREM-2* expression in clusters 1 and 2 that were characterised by expression of the resident KC marker *CD68* and the monocyte marker *CD14* (figure 1F).<sup>25–27</sup> Furthermore, in line with recent work demonstrating the presence of monocyte derived *TREM-2*+*CD9*+ scar-associated macrophages (SAMacs) in human liver cirrhosis,<sup>28</sup> the macrophage cluster was characterised by *CD9* presence (figure 1G). *In silico*-based cellular deconvolution of the RNA-seq TCGA data subsequently correlating *TREM-2* expression with innate and adaptive immune cell gene signatures present in HCC further suggested that in human HCC, *TREM-2* was mainly expressed by macrophages/monocytes as out of the deconvoluted cell types, *TREM-2* positively correlated with macrophages and monocytes but not with *CD4*+ or *CD8*+ T cells nor with neutrophils or endothelial cells (online supplementary table 4). We identified 42 differentially expressed genes between *TREM-2* expressing (clusters 1 and 2; figure 1F), and non-expressing (clusters 0, 3, 4 and 5, figure 1F) tumour infiltrating macrophages (online supplementary figure 6). Gene set enrichment analysis demonstrated enrichment in TLR signalling and lysosome-associated pathways (figure 1H), implying overlapping functions between *TREM-2* expressing tumour infiltrating macrophages and resident *TREM-2* expressing KCs, in the negative regulation of TLR-induced inflammation.<sup>16</sup> Enrichments of lysosome-associated pathways are consistent with recent published observations examining *TREM-2* function in KCs,<sup>29</sup> further suggesting functional similarities between *TREM-2* expressing resident KCs and tumour infiltrating macrophages.



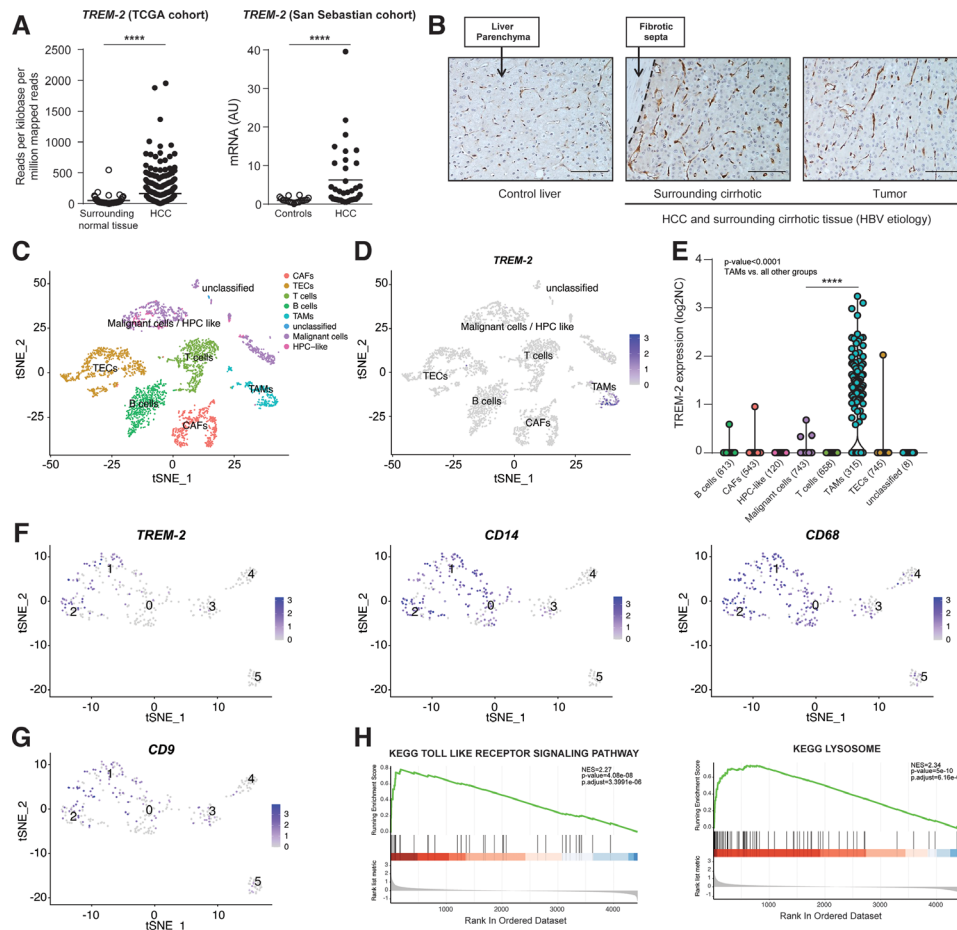


**Figure 1** *TREM-2* expression is elevated in human HCC and is prominently expressed in tumour infiltrating macrophages. (A) qPCR analysis of *TREM-2* expression in surrounding normal tissue and in HCC tissue (n=49 and 366, respectively) in the cohort from TCGA and in normal human liver (controls) and HCC samples (n=21 and 35, respectively) of the San Sebastian cohort. (B) Representative images of *TREM-2* expression by immunohistochemistry in human healthy liver and diseased liver from a patient with an HCC tumour and its surrounding cirrhotic liver of HBV aetiology. Scale bars represent 100  $\mu$ m. (C) t-SNE projection depicting cellular composition of human HCC tumours. Cells that share similar transcriptome profiles are grouped by colours and were annotated using lineage specific markers. (D and E) t-SNE plot depicting *TREM-2* expression in TAMs (D) and corresponding  $\text{Log}_2$  normalised counts ( $\text{Log}_2\text{NC}$ ) *TREM-2* expression values for all tumour infiltrating cells types (E). Shown in brackets are the number of cells analysed for each cell type post-data processing. (F and G) t-SNE projection post-reclustering of TAMs and *TREM-2*, *CD14*, *CD68* (F) and *CD9* (G) expression therein. (H) GSEA plots depicting enrichments in TLR signalling and lysosome pathways within *TREM-2* expressing TAMs. The y-axis represents the enrichment score (ES) and vertical black lines on the x-axis shows where genes annotated to the respective pathways appear in the ranked list of genes. The coloured band represents the ES values (red for positive and blue for negative). (A) Non-parametric Mann-Whitney test was used. (E) One-way analysis of variance followed by Tukey's post-test was used. \*\*\*\*Denotes a p value of <0.0001. AU, arbitrary units, CD, cluster of differentiation, GSEA, gene set enrichment analysis; HCC, hepatocellular carcinoma; qPCR, quantitative PCR; TAMs, tumour-associated macrophages; TCGA, the cancer genome atlas; TLR, Toll-like receptor; *TREM-2*, triggering receptor expressed on myeloid cells 2; tSNE, t-distributed Stochastic Neighbour Embedding.

Together, these observations indicated a particular importance for *TREM-2* expression in tumour infiltrating monocyte-derived macrophages in HCC, suggesting their associated effects with inflammation and fibrosis might be involved in HCC development and/or progression.

### **TREM-2 attenuates oxidative stress, inflammation and hepatocyte damage during the early phases of liver tumourigenesis**

To determine the role of *TREM-2* in the early phases of HCC, we performed the well-established model of acute DEN administration, which provides significant insight into the inflammatory mechanisms at play during HCC.<sup>30,31</sup> We thus acutely injected 8 week-old *Trem-2*<sup>-/-</sup> or WT control mice with 100 mg/kg DEN and humanely sacrificed both genotypes at different time points

(figure 2A). H&E staining revealed more extensive liver damage in *Trem-2*<sup>-/-</sup> versus WT animals, associated with augmented hepatic phospho-histone H2AX ( $\gamma$ H2AX) levels, a surrogate marker for DNA damage (figure 2B, C). Consistently, while there were no baseline differences in circulating alanine aminotransferase (ALT) levels between genotypes, significantly elevated ALT was found in *Trem-2*<sup>-/-</sup> mice post-DEN versus controls (figure 2D). Notably, increased levels of hepatic ROS were observed in *Trem-2*<sup>-/-</sup> compared with WT mice post-DEN (figure 2E). This was associated with increased inflammatory (C-X-C motif chemokine ligand 1 (*Cxcl1*), chemokine (C-C motif) ligand two or monocyte chemoattractant protein 1 (*Mcp1*), tumour necrosis factor (*Tnf*)), mitogenic (hepatocyte growth factor (*Hgf*)) and oxidative stress-related gene expression (*Hmox1* heme oxygenase 1) in *Trem-2*<sup>-/-</sup> compared with WT animals (figure 2F). However, we did not



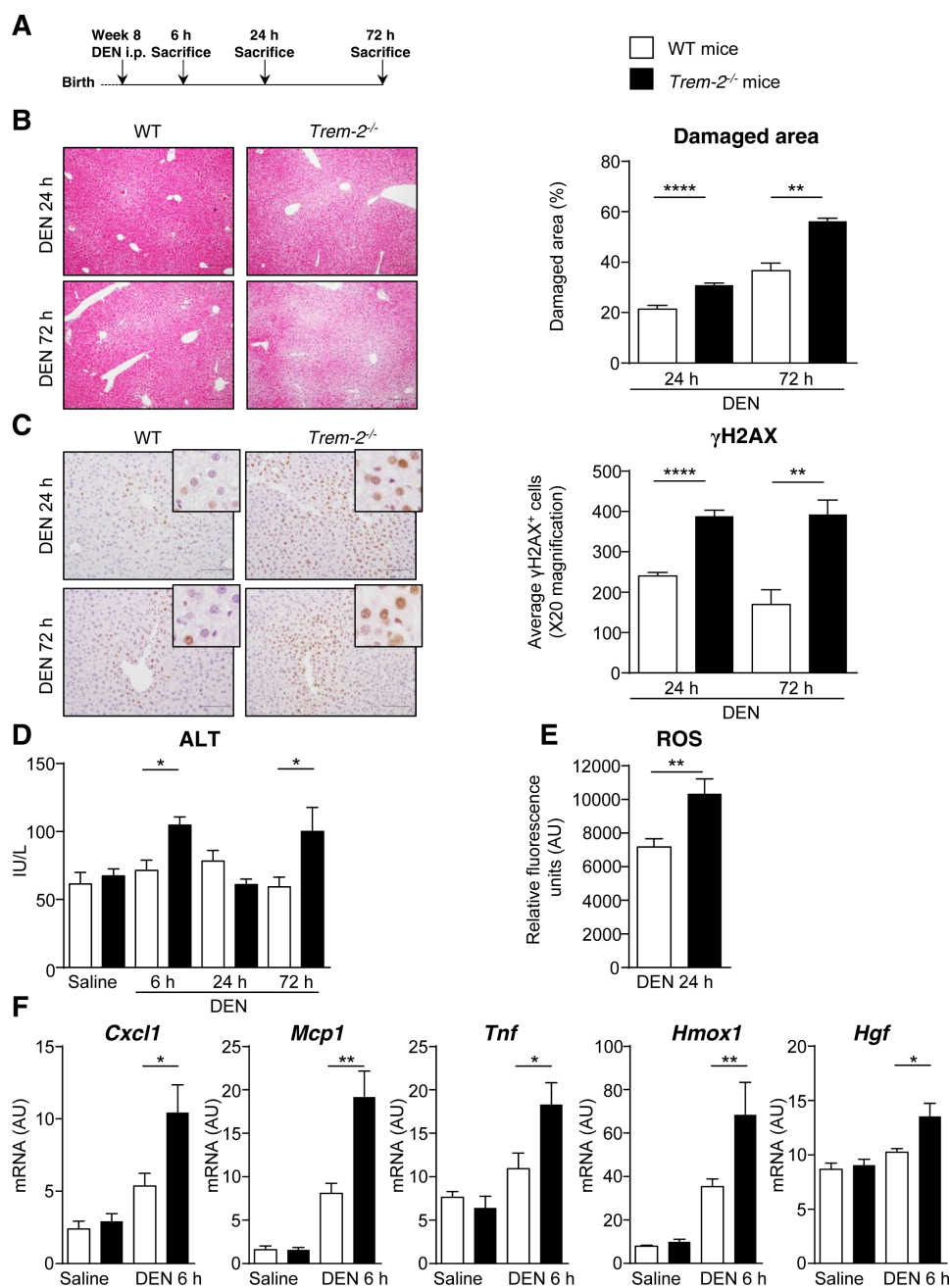


**Figure 2** *Trem-2*<sup>-/-</sup> mice exhibit increased hepatocyte damage, inflammation and oxidative stress in an acute DEN model. (A) Scheme depicting experimental outline of acute DEN in both genotypes of mice following injection with 100 mg/kg DEN (saline; n=6–7, DEN 6 hour; n=7, DEN 24 hours; n=10, DEN 72 hours; n=6–7). (B) Quantification of damaged livers of both genotypes at the indicated time points and representative H&E images. (C) Quantification of damaged hepatocytes at the indicated time points measured by manually counting  $\gamma$ H2AX positive nuclei and representative IHC images. (D) ALT levels were determined in the serum post-DEN. (E) ROS was determined in liver tissue of WT and *Trem-2*<sup>-/-</sup> mice after 24 hours of DEN administration with the H2DCFDA dye. (F) mRNA levels of the chemokines *Cxcl1* and *Mcp1*, the cytokine *Tnf* and the oxidative stress enzyme *Hmox1* and the growth factor *Hgf* were determined. Parametric Student's *t*-test and non-parametric Mann-Whitney test were used. Data represent mean $\pm$ SEM and \*, \*\* and \*\*\*\* denote a p value of <0.05, <0.01 and <0.0001, respectively. ALT, alanine aminotransferase; AU, arbitrary units; *Cxcl1*, C–X–C motif chemokine ligand 1; DEN, diethylnitrosamine; *Hgf*, hepatocyte growth factor; *Hmox1*, heme oxygenase 1; IHC, immunohistochemistry; *Mcp1*, monocyte chemoattractant protein 1; ROS, reactive oxygen species; *Tnf*, tumour necrosis factor; TREM-2, triggering receptor expressed on myeloid cells-2.

observe differences in hepatic immune cell recruitment between genotypes (online supplementary figure 7). These data suggested an importance for TREM-2 in suppressing inflammation, ROS production and consequent liver damage during the initiation of DEN-induced carcinogenesis. To corroborate these findings, we next performed gain-of-function experiments. We intravenously

injected WT C57BL/6 animals with either a control adenovirus or an adenovirus encoding TREM-2 under the transcriptional control of the cytomegalovirus promoter. Seventy-two hours post-virus infection, we acutely injected mice with DEN and evaluated both groups of animals 72 hours post-DEN (figure 3A). Rati-fying transduction efficiency, TREM-2 was robustly expressed

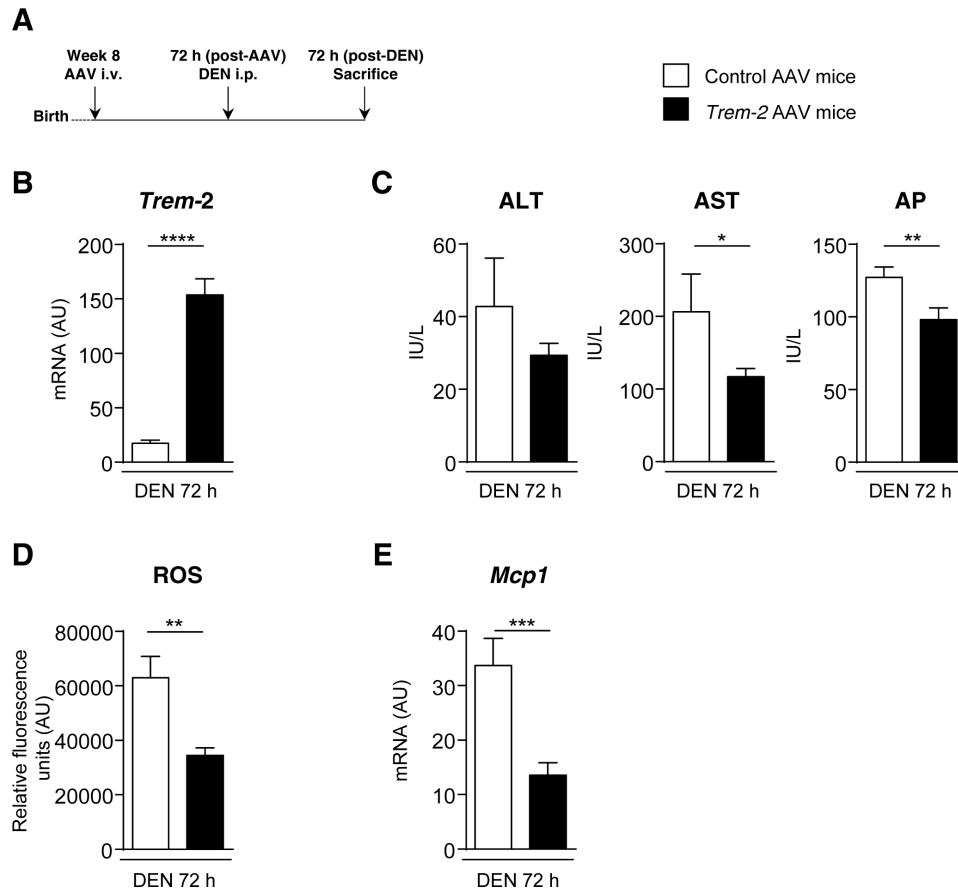


**Figure 3** TREM-2 overexpression lowers liver injury, inflammation and oxidative stress in acute DEN. (A) Scheme depicting experimental outline for TREM-2 overexpression. C57BL/6 mice were intravenously injected with control or TREM-2 expressing adenoassociated viruses ( $1 \times 10^{11}$  pfu) and after 72 hours mice were intraperitoneally injected with 100 mg/kg DEN. Animals were sacrificed 72 hours post-DEN ( $n=10$ ). (B) mRNA levels of *Trem-2*. (C) ALT, AST and AP levels were determined in the serum post-DEN. (D) ROS was determined in liver tissue of C57BL/6 mice 72 hours post-DEN administration with the H2DCFDA dye. (E) mRNA levels of the chemokine *Mcp1* were determined. Parametric Student's *t*-test and non-parametric Mann-Whitney test were used. Data represent mean  $\pm$  SEM and \*, \*\*, \*\*\* and \*\*\*\* denote a *p* value of  $<0.05$ ,  $<0.01$ ,  $<0.001$  and  $<0.0001$ , respectively. AAV, adeno-associated viruses; ALT, alanine aminotransferase; AP, alkaline phosphatase; AST, aspartate aminotransferase; AU, arbitrary units; DEN, diethylnitrosamine; i.p., intraperitoneal; i.v., intravenous; Mcp1, monocyte chemoattractant protein 1; ROS, reactive oxygen species; TREM-2, triggering receptor expressed on myeloid cells 2.

in animals injected with TREM-2 overexpressing *versus* control virus (figure 3B). While there was a slight tendency for ALT levels to be decreased in TREM-2 overexpressing animals opposed to controls, significantly attenuated serum aspartate aminotransferase and alkaline phosphatase levels verified TREM-2 attenuated DEN-mediated liver damage (figure 3C). Importantly, the hepatoprotective effects of TREM-2 overexpression were linked to less ROS and MCP-1 production (figure 3D,E). Thus, complimentary approaches, encompassing animals both genetically lacking and overexpressing TREM-2, demonstrate that it attenuates hepatic damage, inflammation and oxidative stress in the early phases of HCC.

### Trem-2 plays a protective role in HCC

To formally investigate the role of TREM-2 in hepatocarcinogenesis, we next performed a chronic DEN model, where we injected the hepatocarcinogen DEN or saline control to both genotypes and sacrificed them 30 and 40 weeks post-DEN administration (figure 4A). In parallel, as ROS are important for HCC development<sup>32</sup> and we had observed elevated hepatic ROS in *Trem-2* deficient animals (figure 2E), and decreased ROS in those experimentally overexpressing TREM-2 (figure 3D), we

chronically fed both mouse genotypes a diet supplemented with the antioxidant BHA (figure 4B). Opposed to saline controls, hepatic *Trem-2* levels were increased in the non-tumour tissue of DEN-administered mice (figure 4C). Regarding *Trem-2* expression in tumour tissue *versus* matched non-tumour tissue, *Trem-2* was markedly increased in tumour samples, particularly 40 weeks post-DEN (figure 4D). Remarkably, macroscopic liver analysis demonstrated that DEN-administered *Trem-2*<sup>-/-</sup> mice developed more tumours than controls at both time points (figure 4E). Analysis of tumour size revealed that *Trem-2* deficient animals exhibited increased numbers of small ( $\leq 2$  mm) and big ( $\geq 6$  mm) tumours, and more small and medium size (2–6 mm) tumours 30 and 40 weeks post-DEN, respectively (online supplementary figure 8). Notably, BHA administration reversed the elevated tumourigenesis of *Trem-2*<sup>-/-</sup> mice, supporting an involvement of ROS in the protective effects mediated by TREM-2 (figure 4F). Of note, the antioxidant regimen also extensively lowered tumour burden of WT mice, which is consistent with DEN-mediated tumourigenesis being blocked by antioxidants.<sup>30 33</sup>

We next set out to confirm these macroscopic observations and elaborate on the potential mechanisms behind them. H&E staining confirmed increased hepatic tumours in

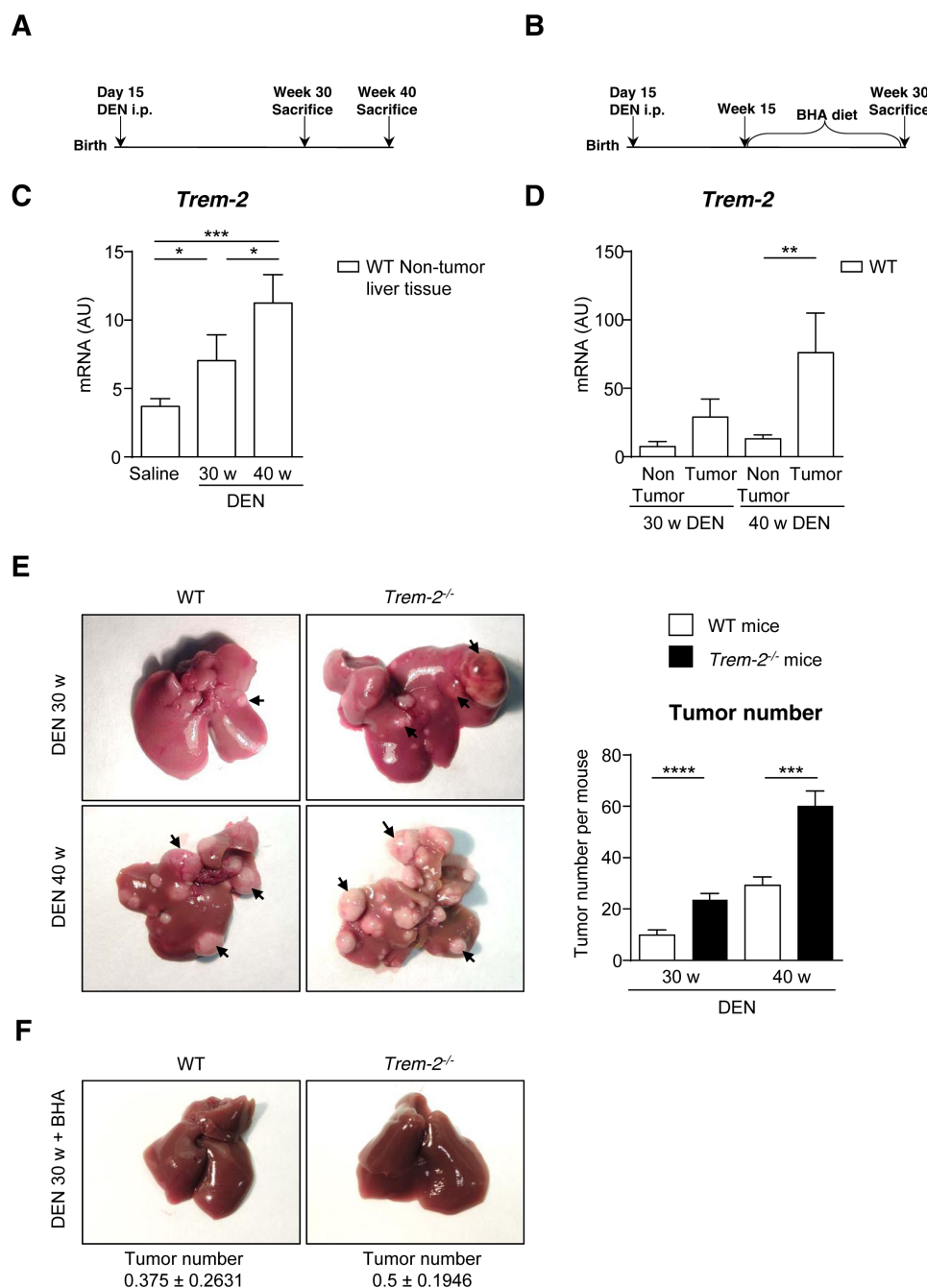


**Figure 4** *Trem-2* null mice exhibit elevated tumorigenesis post-DEN. (A) Scheme depicting experimental outline of chronic DEN in both genotypes of mice following injection with 30 mg/kg DEN (n=14–17). (B) Diagram depicting antioxidant intervention with BHA during chronic DEN (n=7–12). (C) qPCR analysis of hepatic *Trem-2* expression of 30 and 40 weeks DEN-injured mice and (D) qPCR analysis of *Trem-2* expression in non-tumour *versus* tumour tissue in the liver of 30 and 40 weeks DEN-injured mice. (E) Representative pictures of the livers (arrows depict tumours) and total tumour number per mice are shown. (F) Representative liver pictures of DEN injured mice after 15 weeks of BHA diet (n=7–12) and tumour numbers herein. (C-E) Parametric Student's *t*-test and non-parametric Mann-Whitney test were used. Data represent mean±SEM and \*, \*\*, \*\*\* and \*\*\*\* denote a *p* value of <0.05, <0.01, <0.001 and <0.0001. AU, arbitrary units; BHA, butylated hydroxyanisole; DEN, diethylnitrosamine; i.p., intraperitoneal; qPCR, quantitative PCR; TREM-2, triggering receptor expressed on myeloid cells 2; WT, wild type.

*Trem-2*<sup>-/-</sup> animals (figure 5A). To evaluate hepatocyte proliferation in pre-neoplastic surrounding liver tissue, we next measured proliferating cell nuclear antigen (PCNA) expression using IHC. Post-DEN, *Trem-2*<sup>-/-</sup> mice exhibited increased numbers of PCNA-positive hepatocytes in the surrounding tissue *versus* controls, irrespective of time point (figure 5B). Similarly, IHC analysis of  $\gamma$ H2AX revealed an increased number of  $\gamma$ H2AX-positive hepatocytes in *Trem-2*<sup>-/-</sup> livers compared with WT at both time points (figure 5C). Consistent with findings during acute DEN,

evaluating hepatic immune cell recruitment revealed minor differences between genotypes post-DEN (online supplementary figure 9). Furthermore, caspase-3/7 activation and protein levels of the kinase receptor-interacting protein kinase 3 as well as phosphorylation of its downstream substrate mixed lineage kinase domain-like<sup>34</sup> were similar between genotypes 30 and 40 weeks post-DEN (online supplementary figure 10).

In line with ROS playing critical roles in DNA damage and cellular proliferation during HCC,<sup>35</sup> the BHA regimen (figure 4B)



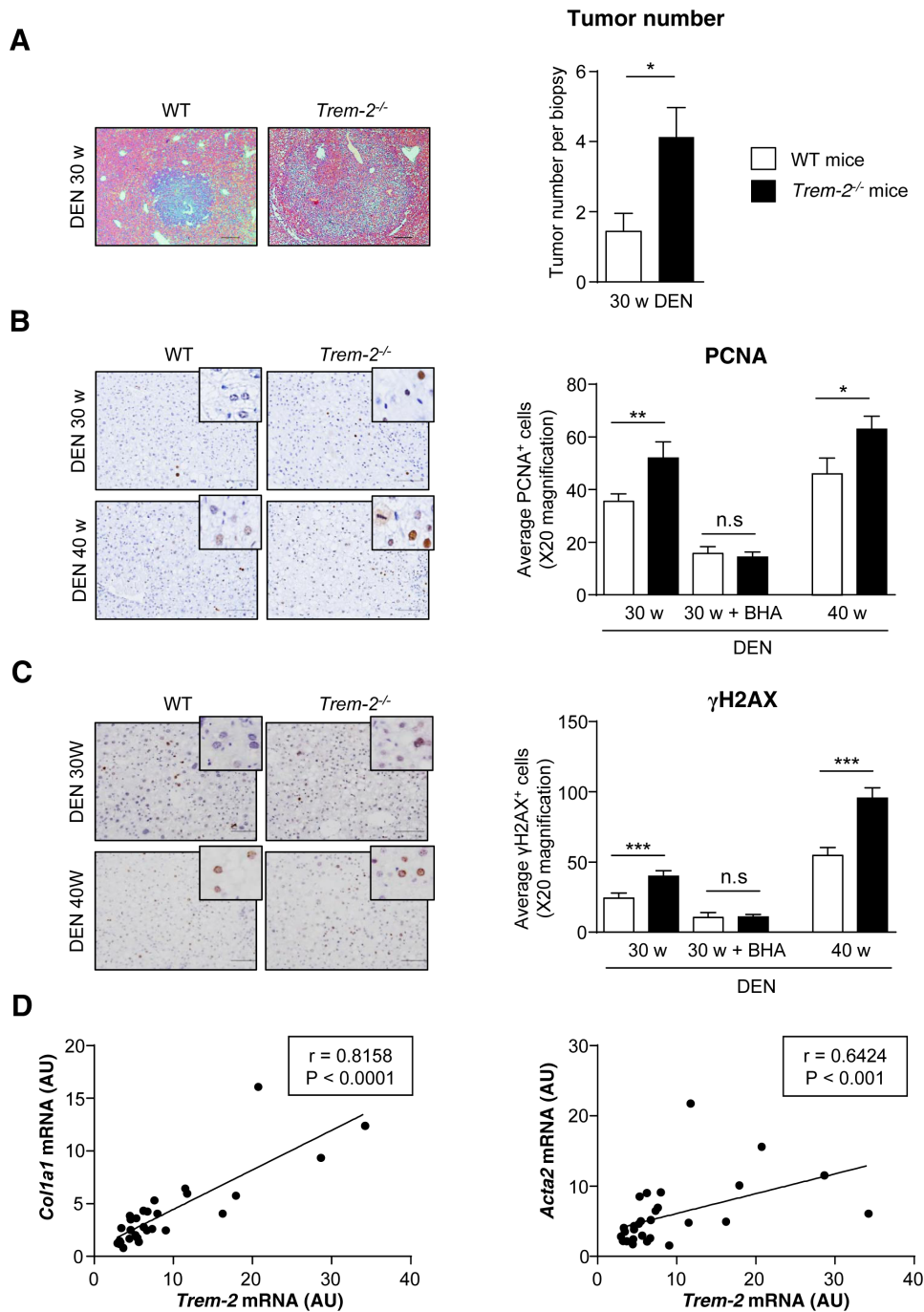


**Figure 5** *Trem-2* null mice exhibit increased numbers of proliferative and damaged hepatocytes post-DEN-induced carcinogenesis. (A) Total HCC tumour counting in DEN-injected WT and *Trem-2<sup>-/-</sup>* livers sacrificed after 30 weeks (n=16). (B and C) Microscopic analysis of WT and *Trem-2<sup>-/-</sup>* mice injected with 30 mg/kg DEN and sacrificed after 30 and 40 weeks fed with a normal or a BHA diet for 15 weeks (n=7–17). (B) Representative PCNA IHC images and quantification of proliferative hepatocytes measured by manually counting PCNA positive nuclei (20×) (C). Representative  $\gamma$ H2AX IHC images and quantification of damaged hepatocytes measured by manually counting  $\gamma$ H2AX positive nuclei (20×). Scale bars represent (A) 1000  $\mu$ m and (B and C) 100  $\mu$ m. (D) Correlation between the mRNA expression levels of *Trem-2* and markers of fibrosis *Col1a1* and *Acta2* in the non-tumour liver tissue of DEN-administered WT mice sacrificed after 30 and 40 weeks (n=29). (A–C) Parametric Student's *t*-test and non-parametric Mann-Whitney test were used. (D) Spearman's correlation test was used. Data represent mean $\pm$ SEM and \*, \*\*, and \*\*\* denote a *p* value of <0.05, <0.01 and <0.001, respectively. AU, arbitrary units; *Acta2*, actin alpha 2, smooth muscle; BHA, butylated hydroxyanisole; *Col1a1*, collagen type I alpha 1 chain; DEN, diethylnitrosamine;  $\gamma$ H2AX, phospho-histone H2A.X; HCC, hepatocellular carcinoma; IHC, immunohistochemistry; n.s, non-significant; PCNA, proliferating cell nuclear antigen; TREM-2, triggering receptor expressed on myeloid cells 2; WT, wild type.

attenuated PCNA and  $\gamma$ H2AX levels in both mouse genotypes and reversed the effects of *Trem-2* abrogation (figure 5B and C). Likely reflective of better HCC outcome in general in the context of antioxidants, levels of certain pro-inflammatory cytokines

including *Tnf* and *Rantes* were attenuated in both genotypes of BHA-treated animals (online supplementary figure 11A). Furthermore, we did not detect any differences in pro-inflammatory cytokines 30 or 40 weeks post-DEN between genotypes (online

supplementary figure 11A). In line with this, no differences in c-jun n-terminal kinase activation were observed between genotypes (online supplementary figure 11B). These data suggested a particular importance for TREM-2 in restraining inflammation during the priming phase of DEN-induced HCC (figure 2F). Consistent with the importance of ROS in TREM-2's protective effects in HCC, 40 weeks post-DEN, we observed a strong tendency ( $p=0.0582$ ) towards higher hepatic inducible nitric oxide synthase (*Inos*) levels in *Trem-2*<sup>-/-</sup> animals (online supplementary figure 12A). As *Inos* is a marker for classically activated M1 macrophages,<sup>36</sup> we next examined whether in chronic DEN, there were any differences in genes associated with alternatively activated M2 macrophages, cells that play a modulatory role in hepatic fibrosis.<sup>36,37</sup> Among the tested markers (*Arg1*, *FIZZ-1* and *CD206*), we could not observe any changes nor were there differences in the pro-fibrogenic mediator *Tgf-β* (online supplementary figure 12B). Despite no influences of TREM-2 on *Tgf-β* in DEN-instigated HCC, based on our published observations demonstrating that TREM-2 is markedly upregulated in activated HSCs<sup>16</sup> and that TREM-2 correlates with collagen levels in human HCC (online supplementary figure 3), we next correlated hepatic *Trem-2* levels with pro-fibrotic markers that are prominent during HSC activation in non-tumour liver tissue of WT mice after DEN administration (30 and 40 weeks). By doing so, we could observe that *Trem-2* levels correlated with *Coll1a1* and *Acta2* levels (figure 5D), suggesting TREM-2 expression within activated HSCs might regulate HCC development and/or progression.

Together, these data indicate that alterations in M1/M2 macrophage polarisation, necroptosis or apoptosis between genotypes do not account for the worsened outcome of TREM-2 deficient mice in HCC. Notably, they further suggest that elevated DNA damage and proliferation mediated through oxidative stress is key to the worsened outcome of *Trem-2*-deficient animals. This hypothesis is supported by proteomic analysis of liver tumour tissue post-DEN. Herein, several proteins were significantly and differentially expressed between genotypes (online supplementary figure 13), and gene ontology analysis revealed enrichment of biological processes including oxidoreductase activity and lipid metabolism (online supplementary table 5).

### TREM-2 exerts tumourigenic protective effects in fibrosis-associated HCC

To strengthen the protective effects of TREM-2 in HCC and to examine its potential impact on fibrosis-associated hepatocarcinogenesis, we next performed two different HCC models. CCl<sub>4</sub> induces hepatic fibrosis and is frequently combined with DEN administration to study fibrosis-associated HCC.<sup>38</sup> We thus combined chronic DEN with 10 weekly CCl<sub>4</sub> injections starting at week 4 and harvested both genotypes at week 30 (figure 6A). DEN/CCl<sub>4</sub> administration led to increased numbers of small ( $\leq 2$  mm) tumours in *Trem-2*<sup>-/-</sup> animals versus controls at 30 weeks (figure 6B), consistent with the effects of DEN alone at this time point (online supplementary figure 8). Evaluating fibrosis using Sirius red staining, surprisingly demonstrated that despite the enhanced tumourigenesis of *Trem-2*<sup>-/-</sup> mice versus controls, these animals displayed less fibrosis (figure 6C). Furthermore, increased PCNA transcription in DEN/CCl<sub>4</sub>-treated *Trem-2*<sup>-/-</sup> animals suggested increased hepatocyte proliferation (figure 6D). As a second model of fibrosis-associated HCC, TAA was administered to both genotypes in drinking water,<sup>38</sup> starting at week 8 of age, and animals harvested 40 weeks post-TAA administration (figure 6E). *Trem-2*-deficient animals exhibited larger tumours

post-TAA versus controls (figure 6F) and akin to the DEN/CCl<sub>4</sub> model, this was associated with attenuated fibrosis and increased PCNA levels (figure 6G,H). Together, these data encompassing diverse murine models unequivocally demonstrate that TREM-2 restrains tumour development and proliferation in HCC. They further suggest that although TREM-2 promotes fibrosis in HCC, these effects are disassociated from HCC development, supporting recent work indicating that the molecular players in fibrosis and HCC can be uncoupled.<sup>39,40</sup>

### Increased hepatocyte proliferation in *Trem-2*<sup>-/-</sup> mice following PHx

Given the importance of liver regenerative mechanisms in HCC,<sup>41</sup> and the elevated hepatocyte proliferation of *Trem-2*-deficient animals versus controls post-DEN as well as in the fibrosis-associated HCC models (figures 5 and 6), we next investigated how TREM-2 impacts hepatocyte proliferation using PHx. We thus subjected both genotypes to ~70% PHx, subsequently sacrificing them at different time points. *Trem-2* levels increased robustly post-PHx, with a peak of expression 48 hours post-surgery relative to sham-operated mice, suggestive of a potential role in liver regeneration (figure 7A). Strikingly, two independent methods of evaluating hepatocyte proliferation (ie, PCNA immunostaining and BRDU incorporation) revealed increased hepatocyte proliferation in *Trem-2*<sup>-/-</sup> versus WT control animals after PHx (figure 7B,C). PCNA immunoblotting confirmed this result (figure 7D). As the priming phase of liver regeneration preceding hepatocyte proliferation is associated with inflammatory cytokine upregulation,<sup>42</sup> we next hypothesised that perhaps during PHx TREM-2's suppressive effects on hepatocyte proliferation was linked to effects of this receptor on early inflammatory events after PHx. Indeed, elevated hepatocyte proliferation of *Trem-2*-deficient animals was associated with an early augmentation of inflammation as revealed by increased levels of pro-inflammatory genes (ie, *Tnf*, *Il6*). Notably, hepatic levels of *Hgf* were also increased early in *Trem-2*<sup>-/-</sup> opposed to WT animals after PHx (figure 7E). As IL-6 activates STAT3 in PHx,<sup>43</sup> levels of phosphorylated STAT3 were analysed by immunoblotting in both genotypes 6 hours post-PHx. Increased *Il6* levels 6 hours post-PHx in *Trem-2* deficient animals did not result in more hepatic STAT3 activation (online supplementary figure 14A). Lipid accumulation during liver regeneration induces transient steatosis and lipids might be used as a source of energy to ensure proper hepatic regeneration and proliferation.<sup>44,45</sup> Considering an enrichment in lipid metabolism-related processes was observed post-DEN in *Trem-2*<sup>-/-</sup> compared with WT animals (online supplementary table 5), we next evaluated hepatic triglyceride content. Compared with control animals, hepatic triglycerides accumulated 6 hours post-PHx, but there were no genotype specific differences (online supplementary figure 14B). Similarly, there were no differences in serum triglycerides post-DEN (online supplementary figure 14C). Thus, TREM-2 restrains hepatocyte proliferation, an effect likely independent of triglyceride production but linked to hepatic inflammation and growth factor production.

### Overexpression of TREM-2 in HSC modulates Wnt ligand secretion and reduces HCC tumourigenicity

Although our single-cell RNA sequencing analysis of human HCC tumour samples demonstrated that TREM-2 is primarily expressed in tumour infiltrated macrophages (figure 1), we previously demonstrated that TREM-2 is robustly expressed in activated human and murine HSCs during liver injury where it serves

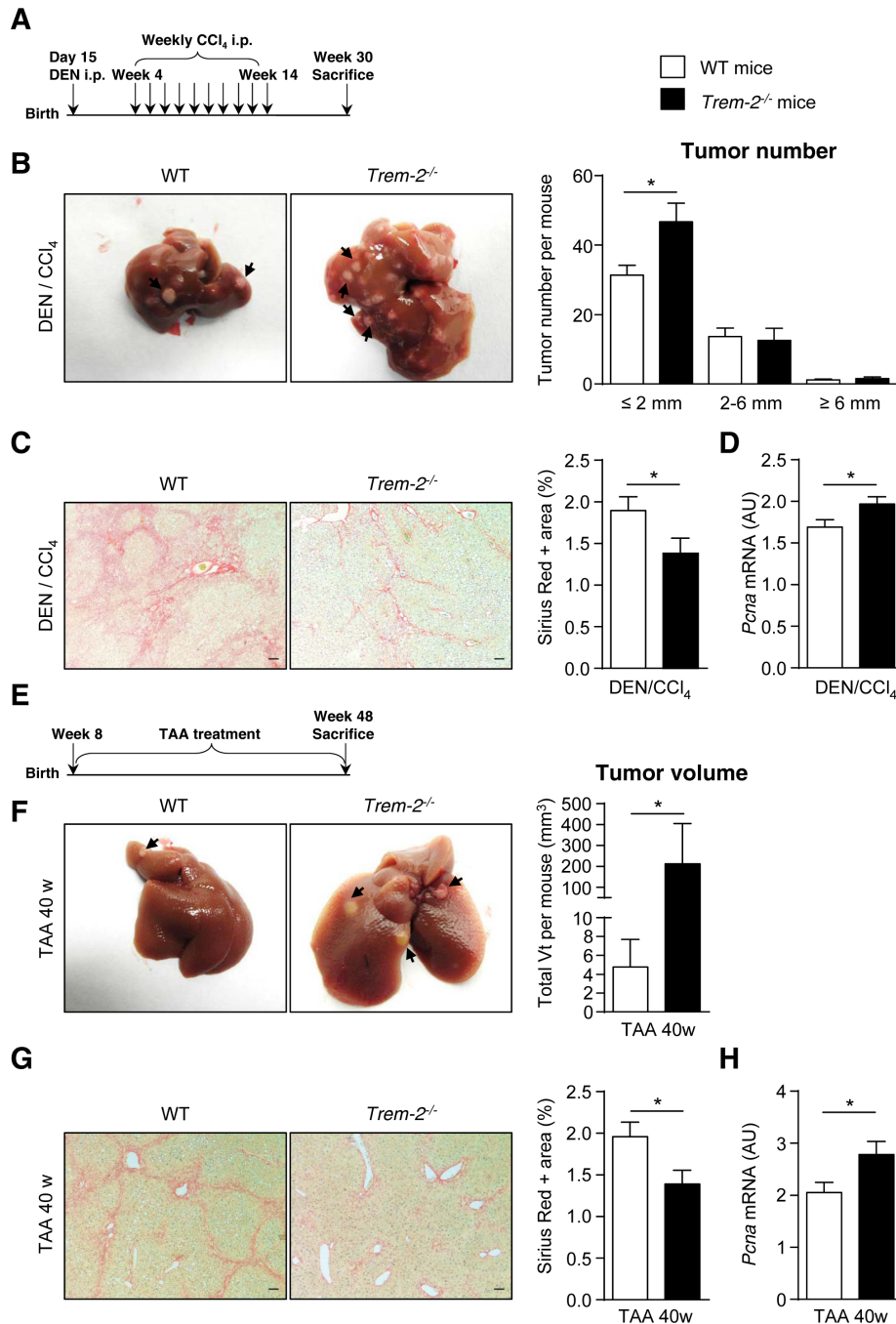


**Figure 6** *Trem-2* null mice exhibit elevated carcinogenesis in fibrosis-associated HCC models. (A–D) WT and *Trem-2*<sup>-/-</sup> mice were injected with 30 mg/kg DEN followed by 10 weekly injections of CCl<sub>4</sub> and sacrificed at 30 weeks post-DEN injection. (A) Scheme depicting experimental outline of DEN/CCl<sub>4</sub> in both genotypes of mice (n=13–14). (B) Representative pictures of the livers (arrows depict tumours) and tumour number classified by size and per mouse are shown. (C) Liver fibrosis was analysed by Sirius red staining. Representative images (4×) and quantification by Image J software (10×) are shown. (D) Hepatic *Pcna* expression by qPCR of DEN/CCl<sub>4</sub> treated WT and *Trem-2*<sup>-/-</sup> mice. (E–H) TAA (0.03% w/v) was administered to WT and *Trem-2*<sup>-/-</sup> mice for 40 weeks. (E) Scheme depicting experimental outline of TAA administration (n=9). (F) Representative pictures of the livers (arrows depict tumours) and total tumour volume (calculated with the formula  $Tv = (W^2 \times L)/2$ ) per mouse are shown. (G) Liver fibrosis was analysed by Sirius red staining; representative images (4×) and quantification by Image J image analysis software (10×) are shown. (H) Hepatic *Pcna* expression by qPCR of WT and *Trem-2*<sup>-/-</sup> mice after TAA administration. Scale bars (C and G) represent 100 μm. Parametric Student's t test and non-parametric Mann-Whitney test were used. Data represent mean±SEM and \* denotes a p value of <0.05. AU, arbitrary units; CCl<sub>4</sub>, carbon tetrachloride; DEN, diethylnitrosamine; HCC, hepatocellular carcinoma; i.p., intraperitoneal; PCNA, proliferating cell nuclear antigen; qPCR, quantitative PCR; TAA, thioacetamide; TREM-2, triggering receptor expressed on myeloid cells 2; WT, wild type.

to modulate TLR-mediated inflammation.<sup>16</sup> It is well established that activated HSCs infiltrate the tumour stroma, secrete extracellular matrix (ECM) proteins and favour HCC tumourigenicity through changes in their secretory phenotype.<sup>46–48</sup> Given

this, together with our aforementioned published work and that *Trem-2* levels in non-tumour liver tissue of WT mice post-DEN correlated with *Col1a1* and *Acta2* levels (figure 5D), we next explored whether HSC expressed TREM-2 might impact HCC



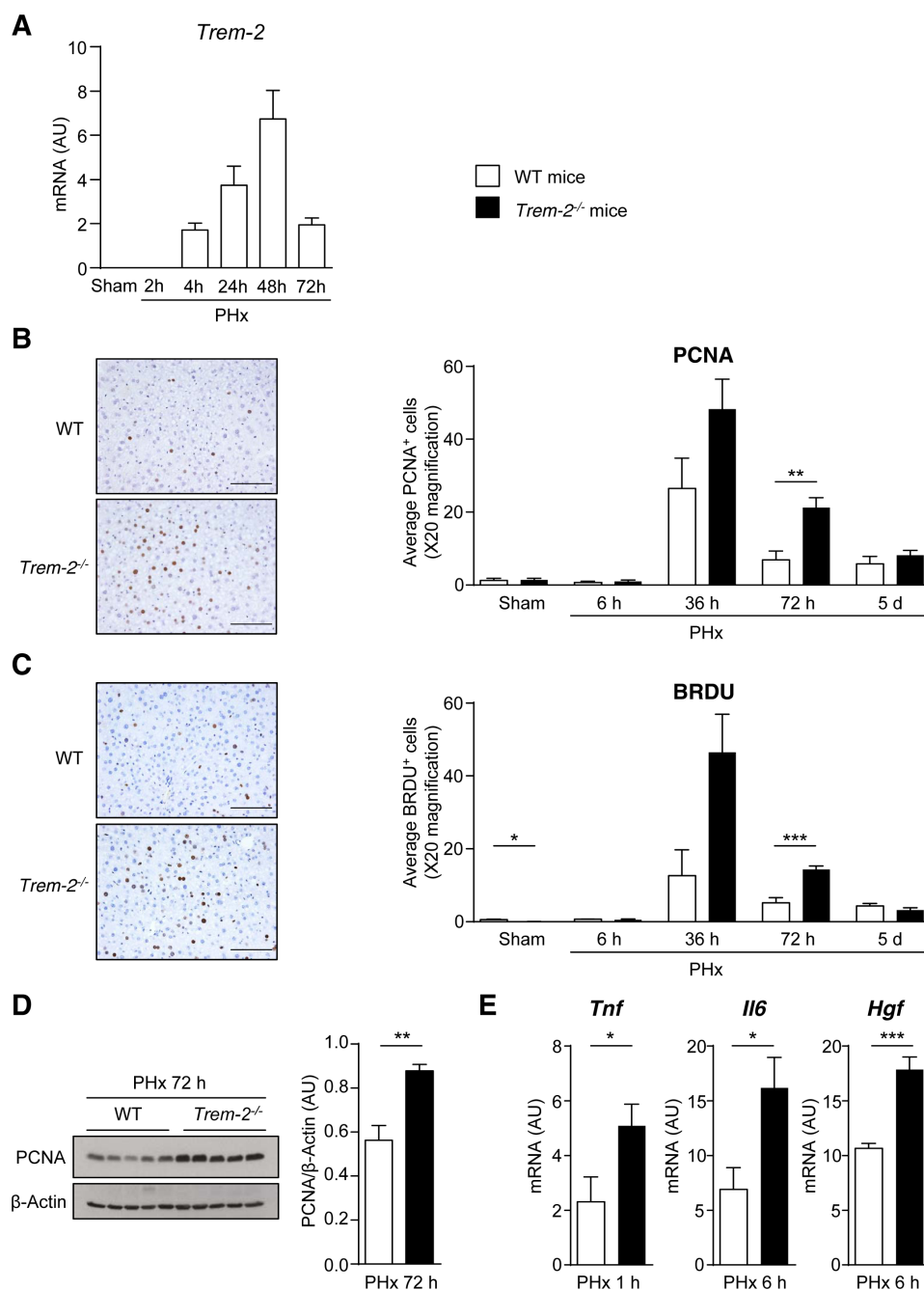


**Figure 7** Role of TREM-2 in liver regeneration and hepatocyte proliferation after PHx. (A) Expression of hepatic *Trem-2* in WT animals at the indicated time points post-PHx (n=3–4). (B–E) WT and *Trem-2*<sup>-/-</sup> mice were sham-operated or subjected to PHx and sacrificed at the indicated time points (n=3–6). (B) Representative IHC images of the PCNA proliferative marker 36 hours post-PHx (20×) and quantification of proliferating hepatocytes measured by counting PCNA positive nuclei. Scale bars represent 100 μm. (C) Representative images of the BRDU staining 36 hours post (20×) and quantification of proliferating hepatocytes measured by manually counting BRDU incorporation in nuclei. Scale bars represent 100 μm. (D) PCNA was determined by immunoblotting 72 hours post-PHx, and β-actin was used as house-keeping control (n=5). Representative images and quantification of the relative PCNA/β-actin levels are shown. (E) mRNA expression of the proinflammatory cytokine *Tnf* 1 hour after PHx (n=5–6), and cytokine *Il6* and *Hgf* 6 hours following PHx (n=6–11). Parametric Student's t test and non-parametric Mann-Whitney test were used. Data represent mean±SEM and \*, \*\*, \*\*\* denote a p value of <0.05, <0.01 and <0.001, respectively. AU, arbitrary units; BRDU, 5'-bromo-2'-deoxyuridine; *Hgf*, hepatocyte growth factor; IHC, immunohistochemistry; *Il6*, interleukin 6, PCNA, proliferating cell nuclear antigen; PHx, partial hepatectomy; *Tnf*, tumour necrosis factor; TREM-2, triggering receptor expressed on myeloid cells 2; WT, wild type.

growth. To evaluate this and translate these findings to the human situation, we next developed a 3D spheroid model. Such models have proved to be invaluable for studying the interactions between cancer cells and their surrounding environment.<sup>49,50</sup> We thus overexpressed TREM-2 in human HSCs (ie, LX-2 cells) *in*

*vitro* and after confirming successful overexpression (figure 8A), carried out culture hanging droplet liver cancer spheroid growth assays with two different HCC cancer cell lines (Hep3B and PLC/PRF5) with the supernatant of these cells *versus* HSCs that had received a control plasmid. Strikingly, supernatant of TREM-2

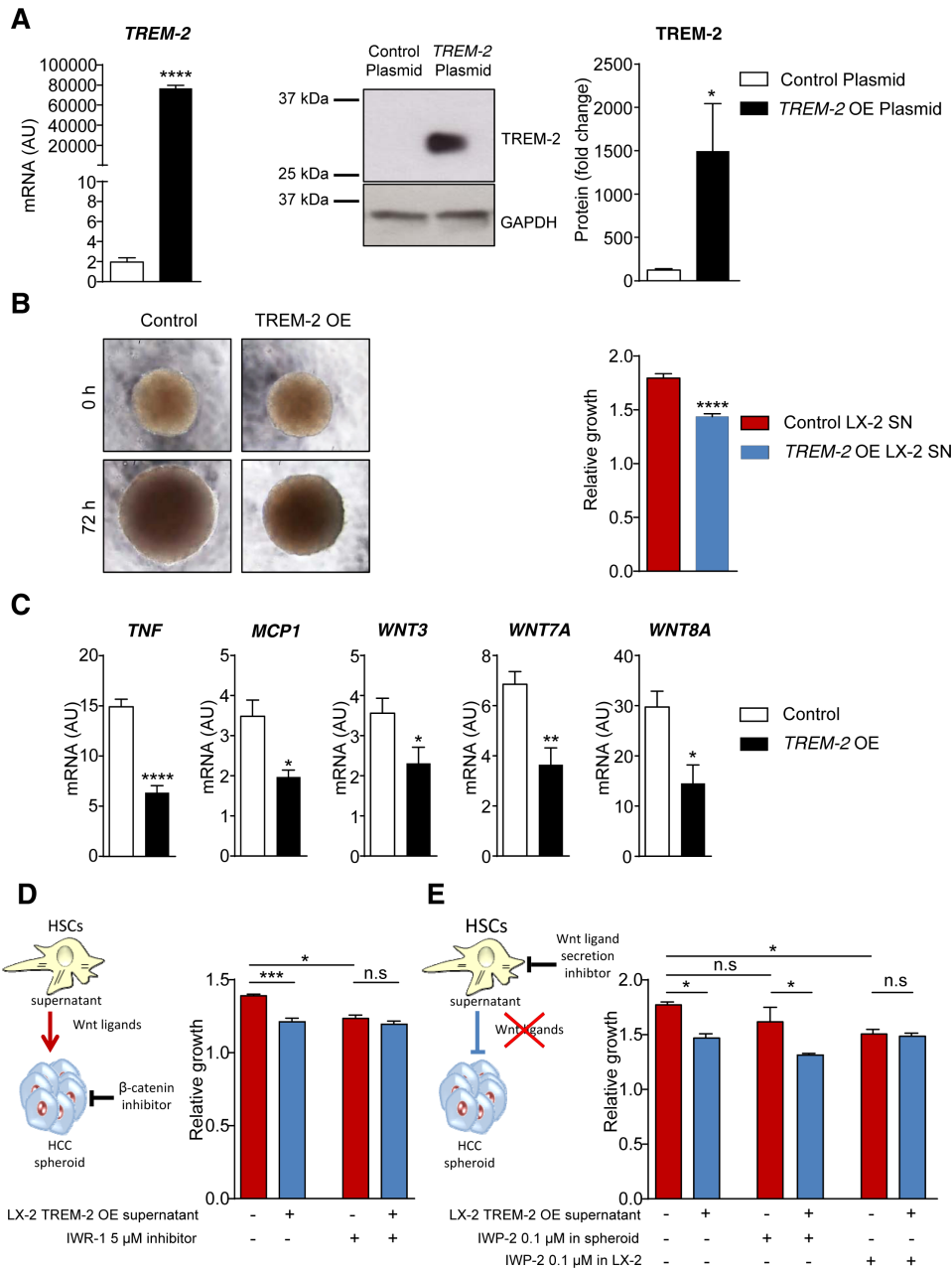


**Figure 8** HCC spheroid culture in LX-2 conditioned media. (A) TREM-2 was overexpressed in LX-2 cells and expression efficiency determined by qPCR and immunoblotting (n=4). (B) Hep3B cells were seeded in hanging droplets for 7 days and forming spheroids were transferred to LX-2 conditioned media from either cells that were overexpressing TREM-2 or a control plasmid. Spheroid size was recorded (20 $\times$ ) using a Nikon eclipse TS100 microscope. (C) *TNF* and *MCP1* and the mRNA levels of canonical Wnt ligands *WNT3*, *WNT7A* and *WNT8A* 24 hours post-TREM-2 overexpression. (D) Hep3B spheroids were incubated with the Wnt/ $\beta$ -catenin inhibitor IWR-1 in LX-2 conditioned media for 72 hours and spheroid growth was recorded as indicated. (E) LX-2 cells or Hep3B spheroids were incubated with the inhibitor of Wnt ligand secretion IWP-2, Hep3B spheroids were incubated in LX-2 conditioned media for 72 hours and spheroid growth was monitored as indicated. (A–C) Parametric Student’s t test and non-parametric Mann-Whitney test were used. (D and E) Kruskal-Wallis test followed by Dunn’s multiple comparison test for individual subgroup comparison was used. Data represent mean $\pm$ SEM and \*, \*\* and \*\*\*\* denote a p value of <0.05, 0.01 and <0.0001, respectively. Data in (A–E) are representative of at least two independent experiments. AU, arbitrary units; GAPDH, glyceraldehyde-3-phosphate dehydrogenase; HCC, hepatocellular carcinoma; HSC, hepatic stellate cells; *MCP1*, monocyte chemoattractant protein 1; n.s, non-significant; OE, overexpression; qPCR, quantitative PCR; SN, supernatant; *TNF*, tumour necrosis factor; TREM-2, triggering receptor expressed on myeloid cells 2.

overexpressing LX-2 cells markedly reduced 3D Hep3B HCC spheroid growth compared with control conditions, suggesting TREM-2 modulated the HSC secretome in a manner that negatively influences HCC proliferation (figure 8B). Similar effects were observed with PLC/PRF5 HCC cells, demonstrating they are not cell-type specific (online supplementary figure 15).

Considering the anti-inflammatory effects of Trem-2 during both PHx (figure 7E) and acute DEN (figure 2F), we next examined whether the aforementioned decreases in HCC spheroid growth instigated by TREM-2 overexpressing HSC supernatant were associated with attenuated basal HSC cytokine expression and secretion. Indeed, both *TNF* and *MCP-1* mRNA and protein

levels in HSCs were attenuated on experimental TREM-2 overexpression (figure 8C, online supplementary figure 16).

Given the major role of the Wnt/ $\beta$ -catenin pathway in HCC<sup>51 52</sup> and that TREM-2 is described to modulate this pathway in other cellular systems including the bone and brain,<sup>53 54</sup> we next evaluated potential effects of TREM-2 on Wnt signalling and HCC growth. TREM-2 overexpression in HSCs attenuated the expression of the canonical Wnt ligands, WNT3, WNT7A and WNT8A suggesting TREM-2 in HSCs might attenuate HCC growth through paracrine Wnt-dependent signalling (figure 8C). To expand on this idea, we next incubated HCC spheroids with TREM-2 overexpressing or control HSC (LX-2) supernatant in the presence or absence of the  $\beta$ -catenin inhibitor IWR-1. Concordant with expression of Wnt ligands in HSCs (figure 8C, white bars), HCC spheroid growth was dependent on Wnt signalling as it was substantially reduced by IWR-1 under control conditions (figure 8D, red bars). Furthermore, the HCC growth-attenuating effect of supernatant from TREM-2 overexpressing HSCs was abolished in IWR-1-treated cells (figure 8D), implicating the effects of TREM-2 on Wnt/ $\beta$ -catenin signalling in HCC growth. Further evidence was obtained from experiments where we blocked Wnt ligand secretion (with the IWP-2 inhibitor) in both sets of HSCs and observed that blocking Wnt ligand secretion abolished the differences associated with TREM-2 overexpression (figure 8E). To rule out potential autocrine effects of IWP-2 treatment on the HCC spheroid (ie, effects of Wnt ligand secretion within the HCC cells), we performed control conditions where in parallel we directly added IWP-2 to HCC spheroids in the presence of supernatant from both sets of HSCs. Strikingly, TREM-2 overexpressing LX-2 supernatant still attenuated HCC growth in these conditions (figure 8E). Together, these data assign a potential function for TREM-2 in influencing the HSC secretome and reducing HCC tumorigenicity via paracrine mechanisms that rely on Wnt signalling.

## DISCUSSION

The role of the immune receptor TREM-2 in human neurodegenerative disorders is currently under intense investigation.<sup>10–12</sup> However, its impact on cancer,<sup>13–15 55</sup> and particularly HCC, is almost unknown. HCC is a common deadly cancer, often arising during chronic liver injury. Therefore, there is an urgent need to identify hepatic anti-inflammatory players and mechanisms regulating hepatocarcinogenesis, as they might represent potential nodes for therapy. We recently reported that TREM-2 is preferentially expressed in non-parenchymal liver cells (ie, KCs and HSCs) acting as a natural inflammation brake during diverse hepatotoxic injuries.<sup>16</sup> Based on these observations, we hypothesised a protective role for TREM-2 in HCC. Here, we found upregulated TREM-2 expression in HCC tissues *versus* control liver tissues. Although high TREM-2 expression in surrounding cirrhotic and HCC tumour tissue *versus* control liver was evident, consistent with published observations indicating TREM-2 is downregulated in patient matched HCC tumour *versus* surrounding tissue,<sup>56</sup> we observed patient-specific heterogeneity, with some patients exhibiting TREM-2 downregulation and others upregulation. Regardless of this heterogeneity, which might be explained by tumour cell biodiversity,<sup>18</sup> here we find that TREM-2 expression in human HCC tumours correlated with markers of inflammation and fibrosis.

HCC usually originates in cirrhosis-associated hepatocellular nodules under regeneration. Here, environmental cues are key and if newly generated hepatocytes are exposed to abnormal

chronic inflammation, normal liver regenerative responses shift towards malignancy linked to excessive hepatic proliferation, genomic instability and tumourigenesis.<sup>57</sup> The early phase of liver regeneration post-PHx is characterised by elevated TNF and IL-6 expression, which are mainly produced by KCs and HSCs.<sup>58</sup> Notably, the expression of these cytokines, as well as *Hgf*, are increased in *Trem-2*<sup>-/-</sup> animals *versus* WT controls after PHx and this is accompanied with increased hepatocyte proliferation. Although TREM-2 negatively regulates TLR4-mediated inflammation in KCs and HSCs, our previous observations demonstrating equivalent inflammation in TNF or IL-1 challenged *Trem-2*<sup>-/-</sup> KCs and HSCs *versus* controls demonstrate that TREM-2 does not directly influence non-parenchymal hepatic cell cytokine signalling.<sup>16</sup> Interestingly, *Tlr4*<sup>-/-</sup> mice display similar regenerative responses post-PHx to WT controls, suggesting lipopolysaccharide signalling is not required for hepatic regenerative responses.<sup>59 60</sup> Similarly opposed to controls, identical hepatic regeneration reportedly occurs in TLR2-deficient and TLR9-deficient animals, indicating that responses to lipoteichoic acid or bacterial DNA, ligands of the aforementioned TLRs whose signalling is modulated by TREM-2, is dispensable for liver regeneration.<sup>3 59–61</sup> Thus TREM-2's suppressive effects on hepatocyte proliferation might occur following engagement of multiple TLR ligands. Alternatively, TREM-2 could impact hepatic regenerative responses TLR independently, possibly through its postulated ligands that include phospholipids, proteoglycans, apolipoproteins and heat shock protein 60.<sup>6–9</sup> Interestingly, several of these are associated with regenerative responses either in the liver or in other systems and organisms.<sup>45 62 63</sup> Regardless of the exact upstream mechanism, our PHx data support the notion that TREM-2's effects on inflammation and growth factor production are intertwined with hepatic regenerative responses.

The tumour microenvironment plays a fundamental role in HCC development and progression, and comprises inflammatory cytokines, growth factors, proteolytic enzymes, non-parenchymal hepatic cells, immune cells and ECM proteins.<sup>48</sup> While during murine HCC we observed no impact of TREM-2 on immune cell recruitment, hepatic *Trem-2* levels correlated with HSC activation in surrounding non-tumour liver tissue, consistent with the idea that in mice TREM-2-expressing activated HSCs infiltrate the tumour microenvironment. However, in fibrosis-associated HCC models, opposed to controls, *Trem-2*<sup>-/-</sup> animals exhibited attenuated fibrosis associated with augmented tumourigenesis. Although this might seem counterintuitive, as fibrosis is a strong risk factor for HCC, importantly these data are consistent with seminal recent single-cell RNA sequencing work demonstrating a pro-fibrogenic role for TREM-2+CD9+ expressing monocyte derived SAMacs in both human and murine CCl<sub>4</sub>-induced liver cirrhosis.<sup>28</sup> Conditioned media from primary human TREM-2 expressing SAMacs, which interestingly exhibits high baseline IL-1 $\beta$  and IL-8 production, promotes collagen expression in primary human HSCs.<sup>28</sup> In agreement with this, we observed high TREM-2 expression in cells both infiltrating tumours and inflammatory periportal areas in the surrounding cirrhotic tissue. Furthermore, TREM-2 expression positively correlated with *COL1A1*, *IL1B* and *IL8* levels. Importantly, our single-cell RNA sequencing analysis was able to expand on these recent findings by demonstrating the presence of infiltrated TREM-2 expressing monocyte-derived macrophages in human HCC tumours that were also CD9+ and CD68+, suggesting they resemble SAMacs. Although, we did not examine TREM-2+CD9+ monocyte-derived macrophage presence in murine HCC tumours, given their recently published



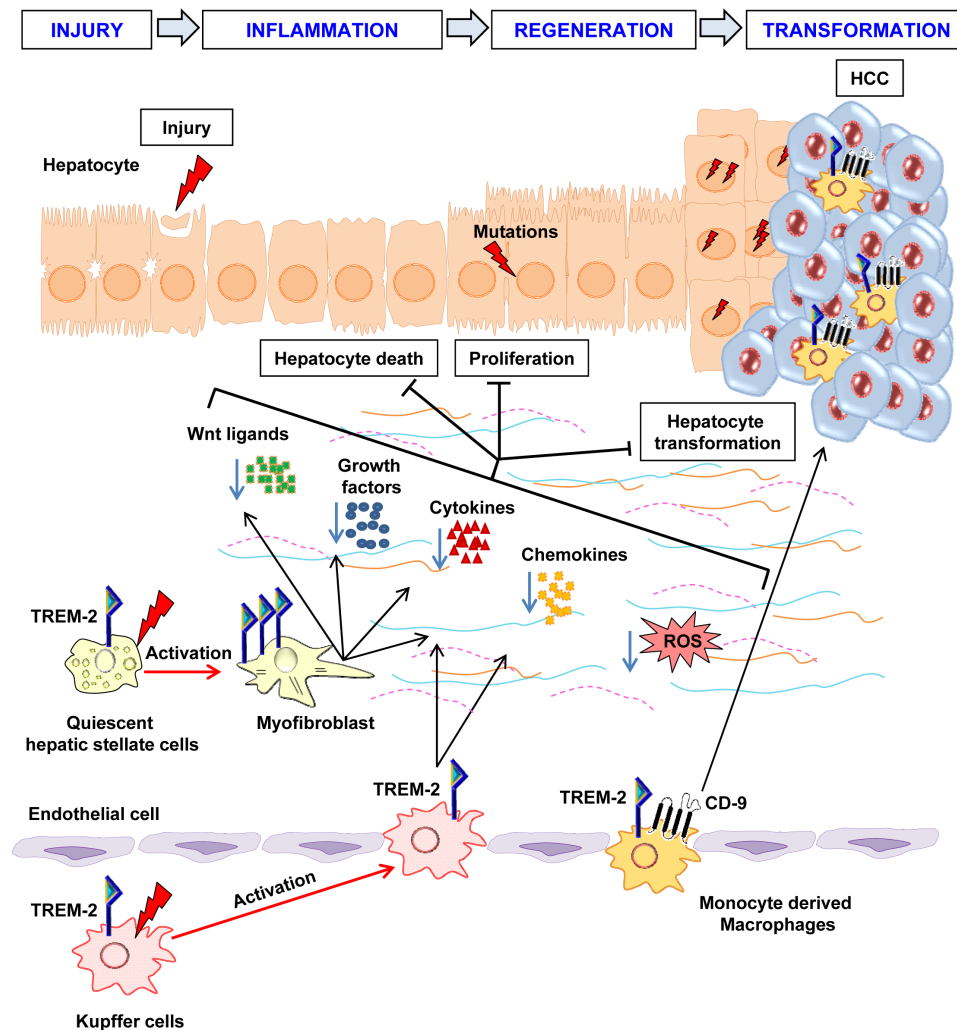


**Figure 9** TREM-2 modulates hepatocarcinogenesis in a multifactorial manner. Post-liver damage, *Trem-2* absence leads to elevated DNA damage and hepatocyte death which provokes further DNA damage and augments inflammation and growth factor production. Conversely overexpression of TREM-2 dampens hepatic damage, inflammation and ROS, suggesting endogenous TREM-2 modulates hepatocellular injury in the initiation phase of HCC. TREM-2 expression in HSCs further impacts WNT ligand and cytokine expression/secretion, which impacts HCC growth. Recruitment of TREM-2+CD9+ monocyte-derived macrophages into HCC tumours is also depicted. Although the exact function of these cells remains to be elucidated, they are likely functionally similar to TREM-2 expressing KCs. Together, TREM-2's expression in non-parenchymal and infiltrating cells and its associated effects may impact the mutational rate of proliferating hepatocytes, altering hepatocyte regeneration, transformation and dampening HCC development. HCC, hepatocellular carcinoma; ROS, reactive oxygen species; TREM-2, triggering receptor expressed on myeloid cells 2.

presence and profibrogenic role in murine CCl<sub>4</sub> fibrosis,<sup>28</sup> the absence of fibrosis in *Trem-2*<sup>-/-</sup> versus control animals in the fibrosis-associated hepatocarcinogenesis models makes sense. These findings also support the concept of an uncoupling between the molecular players in fibrosis and HCC.<sup>39 40</sup>

While the ontogeny of human hepatic macrophages is unknown, in mice, embryonic self-renewing tissue-resident KCs predominate in homeostasis but post-injury, hepatic macrophages derived from circulating monocytes accumulate.<sup>64 65</sup> Interestingly, in the naïve state, two murine KC populations have recently been reported, *Trem-2*<sup>lo</sup> and *Trem-2*<sup>hi</sup>, with the *Trem-2*<sup>hi</sup> population predominating in nonalcoholic steatohepatitis models where it is characterised by acquisition of CD9.<sup>29</sup> Furthermore, we previously demonstrated that TREM-2 dampened murine CCl<sub>4</sub>-associated liver injury partly through ROS production within injury-associated inflammatory monocyte-derived macrophages, the recruitment of which depended on TLR4-driven inflammation within HSCs.<sup>16</sup> Given that TREM-2 attenuates hepatic damage, inflammation and oxidative stress in

the early phases of HCC (figure 3), we hypothesise that HSC or KC expressed TREM-2 serves to dampen infiltration of TREM-2+CD9+ monocyte-derived macrophages in HCC tumours. Although, the relative contribution of these cells to murine and human HCC remains to be determined, here we find that (1) human HCC tumours are rich in TREM-2 expressing monocyte-derived macrophages; (2) Akin to reported effects of TREM-2 expression in KCs, TREM-2 expression in tumour-infiltrated macrophages is associated with TLR signalling and lysosomal pathways<sup>16 29</sup>; (3) TREM-2 expression in human HCC tumours correlates with inflammation; (4) overexpression of TREM-2 in human HSCs dampens MCP-1 levels and (5) TREM-2 unequivocally plays a protective role in hepatocarcinogenesis.

Interestingly, conditioned media of TREM-2 overexpressing HSCs but not control HSCs inhibited HCC spheroid growth and this was also associated with reduced expression of TNF, MCP1 and canonical Wnt ligands. Blocking Wnt ligand secretion in HSCs abrogated the reduced HCC growth associated with HSC TREM-2 overexpression, adding influences of canonical Wnt

signalling to part of TREM-2's 'protective network' during HCC. These data are consistent with the critical role of  $\beta$ -catenin activation in liver tumourigenesis and its frequent reactivation in HCC.<sup>51,52</sup> They also underscore the importance of the microenvironment and the tumour promoting effects of HSCs. HSC activation is critical for hepatic tumourigenesis as cotransplantation of only activated HSCs with HCC cells into nude mice promotes tumour growth, an effect partly dependent on HGF.<sup>46,66</sup> Here, we demonstrate that in HCC, hepatic *Trem-2* levels correlated with HSC activation in the tumour microenvironment and that *Hgf* is suppressed by TREM-2 during regeneration.

Nonetheless, the protective effects of TREM-2 were apparent at many levels including inflammation, ROS and growth factor production. In this regard, ROS are described to modulate Wnt, growth factor signalling and inflammation.<sup>67,68</sup> Administration of antioxidant diets to mice inhibits DEN-mediated hepatocarcinogenesis by reducing ROS and ROS-mediated DNA damage.<sup>30,33</sup> Our data demonstrating that the antioxidant BHA is able to almost completely block DEN-induced hepatocarcinogenesis in both genotypes is consistent with these reports, and additionally connects the suppressive effects of TREM-2 on ROS to dampened hepatocyte proliferation and damage. While, admittedly we cannot pinpoint what is the most important contributing effect of TREM-2 to HCC protection, we provide solid evidence that TREM-2 exerts multiple biological effects that likely together contribute to decreased HCC pathogenesis. Our work is also in line with previous observations indicating that the proinflammatory receptor TREM-1, which exerts opposing functions to TREM-2,<sup>5</sup> is detrimental in HCC.<sup>31</sup> Despite this, we are hesitant to conceptually label TREM-2 as a 'tumour suppressor' in HCC.<sup>56</sup> In this regard, we and others have shown that TREM-2 is not expressed in mouse hepatocytes and here we observe no TREM-2 expression on transformed human hepatocytes, suggesting insignificant effects of hepatocyte TREM-2 deficiency to the murine DEN model.<sup>16,69</sup> Furthermore, to our knowledge, unlike classic tumour suppressor genes such as p53,<sup>70</sup> there are no published genome wide association studies supporting that rare TREM-2 variants are associated with HCC risk. Rather, such studies have conclusively demonstrated links with Alzheimer's disease.<sup>10</sup>

In summary, all these data indicate that TREM-2 plays a critical role during hepatocarcinogenesis, negatively regulating liver inflammation, oxidative stress and Wnt ligand secretion (figure 9). In this context, TREM-2 prevents hepatocyte proliferation and damage, and consequently HCC development and growth. Thus, by exerting suppressive effects on diverse HCC promoting processes, non-parenchymal TREM-2 represents a central hub that is relevant and critical for HCC pathogenesis. In this regard, the future determination of the TREM-2 ligands will open new avenues for therapeutic interventions. Moreover, our results suggest an importance for investigating TREM-2 agonists. Although cell-type specific TREM-2 agonism is likely challenging, hepatic TREM-2 agonism would presumably attenuate inflammation and oxidative stress in both non-parenchymal hepatic stromal cells and tumour infiltrating monocyte-derived macrophages. Thereby, although, it may prevent hepatocyte damage, proliferation and impact HCC tumour burden in a multifactorial manner, it might be associated with unwarranted effects on fibrosis.

#### Author affiliations

<sup>1</sup>Department of Liver and Gastrointestinal Diseases, Biodonostia Health Research Institute, Donostia University Hospital, San Sebastian, Spain

<sup>2</sup>Institute for Vascular Biology, Center for Physiology and Pharmacology, Medical University Vienna, Vienna, Austria

<sup>3</sup>Christian Doppler Laboratory for Arginine Metabolism in Rheumatoid Arthritis and Multiple Sclerosis, Vienna, Austria

<sup>4</sup>Newcastle Fibrosis Research Group, Institute of Cellular Medicine, Faculty of Medical Sciences, Newcastle University, Newcastle upon Tyne, United Kingdom

<sup>5</sup>CIBERehd, Instituto de Salud Carlos III (ISCIII), Madrid, Spain

<sup>6</sup>Department of Health and Medical Sciences, Biotech Research & Innovation Centre (BRIC), University of Copenhagen, Copenhagen, Denmark

<sup>7</sup>Biochemistry Department, Faculty of Pharmacy, Minia University, Minya, Egypt

<sup>8</sup>Proteomics Platform, CIC bioGUNE, ProteoRed-ISCIII, Bizkaia Science and Technology Park, Derio, Spain

<sup>9</sup>Department of Physiology, Faculty of Medicine and Nursing, University of the Basque Country, UPV/EHU, Lejona, Spain

<sup>10</sup>CeMM, Research Center for Molecular Medicine of the Austrian Academy of Sciences, Vienna, Austria

<sup>11</sup>Department of Medicine I, Laboratory of Infection Biology, Medical University of Vienna, Vienna, Austria

<sup>12</sup>Department of Medicine, Faculty of Medicine and Nursing, University of the Basque Country, UPV/EHU, Lejona, Spain

<sup>13</sup>IKERBASQUE, Basque Foundation for Science, Bilbao, Spain

**Twitter** Andrea Vogel @andvoege and Jesper B Andersen @jaboeje

**Acknowledgements** The authors thank the staff of the animal facility, the histology platform at the Biodonostia Health Research Institute and Maialen Arruti Martin from the Molecular Pathology Department of Donostia University Hospital for technical assistance. CIC bioGUNE is recipient of Severo Ochoa Excellence Accreditation by MINECO (SEV-2016-0644). The results published here are in part based upon data generated by the TCGA Research Network: <https://www.cancer.gov/tcga>. Furthermore, single-cell RNA sequencing analysis was performed on Gene Expression Omnibus data set GSE125449.

**Contributors** MJP and JMB conceived, designed and coordinated the experiments. AE-B, IL, OS, AA-L, FO, PMR, EH, RJ-A, IR, AL, ALC, MYWZ, PM-G, MA, FE and MJP performed the experiments and obtained the data. AE-B, IL, OS, AA-L, FO, PMR, CJO'R, PM-G, AV, GS, PA, JBA, SK, DAM, LB, JMB and MJP analysed and interpreted the data. EZ, CJO'R and JBA analysed single-cell RNA sequencing data and performed cellular deconvolution and correlation analysis. AE-B, IL, OS, JMB and MJP wrote the manuscript. OS, SK, DAM, LB, JMB and MJP obtained funding. All authors read and approved the final manuscript.

**Funding** Spanish Ministry of Economy and Competitiveness and 'Instituto de Salud Carlos III' grants (MJP (PI14/00399, PI17/00022 and Ramon y Cajal Programme RYC-2015-17755); JMB (PI12/00380, PI15/01132, PI18/01075, Miguel Servet Programme CON14/00129 and CPII9/00008) cofinanced by 'Fondo Europeo de Desarrollo Regional' (FEDER); CIBERehd: MJP, JMB and LB), Spain; IKERBASQUE, Basque foundation for Science (MJP and JMB), Spain; 'Diputación Foral de Gipuzkoa' (MJP: DFG18/114, DFG19/081; JMB: DFG15/010, DFG16/004); BIOEF (Basque Foundation for Innovation and Health Research: EITB Maratoia BIO15/CA/016/BD to JMB); Department of Health of the Basque Country (MJP: 2015111100 and 2019111024; JMB: 2017111010), Euskadi RIS3 (JMB: 2016222001, 2017222014, 2018222029, 2019222054, 2020333010) Department of Industry of the Basque Country (JMB: Elkartek: KK-2020/00008) and AECC Scientific Foundation (JMB). AE-B was funded by the University of the Basque Country (UPV/EHU) (PIF2014/11) and by the short-term training fellowship Andrew K Burroughs (European Association for the Study of the Liver, EASL). IL and AA-L were funded by the Department of Education, Language Policy and Culture of the Basque Government (PRE\_2016\_1\_0152 and PRE\_2018\_1\_0184). OS and SK were funded by the Austrian Science Fund (FWF25801-B22, FWF-P35168 to OS and L-Mac: F 6104-B21 to SK). FO and DAM were funded by a UK Medical Research Council programme Grant MR/R023026/1. DAM was also funded by the CRUK programme grant C18342/A23390, CRUK/AECC/AIRC Accelerator Award A26813 and the MRC MICA programme grant MR/R023026/1. JBA is supported by the Danish Medical Research Council, Danish Cancer Society, Nordisk Foundation, and APM Foundation. CJO'R and PM-G are supported by Marie Skłodowska-Curie Programme and EASL Sheila Sherlock postdoctoral fellowships.

**Competing interests** None declared.

**Patient and public involvement** Patients and/or the public were not involved in the design, or conduct, or reporting or dissemination plans of this research.

**Patient consent for publication** Not required.

**Ethics approval** Samples and clinicopathological information were obtained from the Basque Biobank. Samples were processed following standard operation procedures with appropriate approval of the Clinical Research Ethics Committees of the Basque Country and Donostia University Hospital. An informed consent was obtained from all subjects. Clinical Research Ethics Committees of the Basque Country CEIC-E and Donostia University Hospital. ID: PI+CES-BIOEF 2015-01 14-81.

**Provenance and peer review** Not commissioned; externally peer reviewed.

**Data availability statement** Data are available upon reasonable request. Email address: matxus.perugorria@biodonostia.org.

**Open access** This is an open access article distributed in accordance with the Creative Commons Attribution Non Commercial (CC BY-NC 4.0) license, which permits others to distribute, remix, adapt, build upon this work non-commercially, and license their derivative works on different terms, provided the original work is properly cited, appropriate credit is given, any changes made indicated, and the use is non-commercial. See: <http://creativecommons.org/licenses/by-nc/4.0/>.

#### ORCID iDs

Marco Y W Zaki <http://orcid.org/0000-0003-3097-5776>

Andrea Vogel <http://orcid.org/0000-0002-2613-140X>

Jesper B Andersen <http://orcid.org/0000-0003-1760-5244>

Jesus Maria Banales <http://orcid.org/0000-0002-5224-2373>

Maria Jesus Perugorria <http://orcid.org/0000-0002-7636-0972>

#### REFERENCES

- Forner A, Reig M, Bruix J. Hepatocellular carcinoma. *Lancet* 2018;391:1301–14.
- Aravalli RN. Role of innate immunity in the development of hepatocellular carcinoma. *World J Gastroenterol* 2013;19:7500–14.
- Turnbull IR, Gilfillan S, Cella M, et al. Cutting edge: TREM-2 attenuates macrophage activation. *J Immunol* 2006;177:3520–4.
- Hamerman JA, Jarjoura JR, Humphrey MB, et al. Cutting edge: inhibition of TLR and FcR responses in macrophages by triggering receptor expressed on myeloid cells (TREM)-2 and DAP12. *J Immunol* 2006;177:2051–5.
- Sharif O, Knapp S. From expression to signaling: roles of TREM-1 and TREM-2 in innate immunity and bacterial infection. *Immunobiology* 2008;213:701–13.
- Yeh FL, Wang Y, Tom I, et al. Trem2 binds to apolipoproteins, including APOE and CLU/APOJ, and thereby facilitates uptake of amyloid-beta by microglia. *Neuron* 2016;91:328–40.
- Kober DL, Alexander-Brett JM, Karch CM, et al. Neurodegenerative disease mutations in TREM2 reveal a functional surface and distinct loss-of-function mechanisms. *Elife* 2016;5:e20391.
- Stefano L, Racchetti G, Bianco F, et al. The surface-exposed chaperone, hsp60, is an agonist of the microglial TREM2 receptor. *J Neurochem* 2009;110:284–94.
- Wang Y, Cella M, Mallinson K, et al. Trem2 lipid sensing sustains the microglial response in an Alzheimer's disease model. *Cell* 2015;160:1061–71.
- Jonsson T, Stefansson H, Steinberg S, et al. Variant of TREM2 associated with the risk of Alzheimer's disease. *N Engl J Med* 2013;368:107–16.
- Ulland TK, Song WM, Huang SC-C, et al. Trem2 maintains microglial metabolic fitness in Alzheimer's disease. *Cell* 2017;170:649–63. e13.
- Poliani PL, Wang Y, Fontana E, et al. Trem2 sustains microglial expansion during aging and response to demyelination. *J Clin Invest* 2015;125:2161–70.
- Zhang X, Wang W, Li P, et al. High TREM2 expression correlates with poor prognosis in gastric cancer. *Hum Pathol* 2018;72:91–9.
- Wang X-Q, Tao B-B, Li B, et al. Overexpression of TREM2 enhances glioma cell proliferation and invasion: a therapeutic target in human glioma. *Oncotarget* 2016;7:2354–66.
- Zhang H, Sheng L, Tao J, et al. Depletion of the triggering receptor expressed on myeloid cells 2 inhibits progression of renal cell carcinoma via regulating related protein expression and PTEN-PI3K/Akt pathway. *Int J Oncol* 2016;49:2498–506.
- Perugorria MJ, Esparza-Baquera A, Oakley F, et al. Non-Parenchymal TREM-2 protects the liver from immune-mediated hepatocellular damage. *Gut* 2019;68:533–46.
- Cancer Genome Atlas Research Network. Electronic address: wheeler@bcm.edu, Cancer Genome Atlas Research Network. Comprehensive and integrative genomic characterization of hepatocellular carcinoma. *Cell* 2017;169:1327–41. e23.
- Ma L, Hernandez MO, Zhao Y, et al. Tumor cell biodiversity drives microenvironmental reprogramming in liver cancer. *Cancer Cell* 2019;36:418–30.
- Ebrahimkhani MR, Oakley F, Murphy LB, et al. Stimulating healthy tissue regeneration by targeting the 5-HT<sub>2B</sub> receptor in chronic liver disease. *Nat Med* 2011;17:1668–73.
- Faustino-Rocha A, Oliveira PA, Pinho-Oliveira J, et al. Estimation of rat mammary tumor volume using caliper and ultrasonography measurements. *Lab Anim* 2013;42:217–24.
- Wang X, Wang Q. Alpha-Fetoprotein and hepatocellular carcinoma immunity. *Can J Gastroenterol Hepatol* 2018;2018:9049252:1–8.
- Ohguchi S, Nakatsukasa H, Higashi T, et al. Expression of alpha-fetoprotein and albumin genes in human hepatocellular carcinomas: limitations in the application of the genes for targeting human hepatocellular carcinoma in gene therapy. *Hepatology* 1998;27:599–607.
- Lee TKW, Castilho A, Cheung VCH, et al. CD24(+) liver tumor-initiating cells drive self-renewal and tumor initiation through STAT3-mediated NANOG regulation. *Cell Stem Cell* 2011;9:50–63.
- Han X, Wang Y, Pu W, et al. Lineage Tracing Reveals the Bipotency of SOX9<sup>+</sup> Hepatocytes during Liver Regeneration. *Stem Cell Reports* 2019;12:624–38.
- Kuang D-M, Zhao Q, Peng C, et al. Activated monocytes in peritumoral stroma of hepatocellular carcinoma foster immune privilege and disease progression through PD-L1. *J Exp Med* 2009;206:1327–37.
- Wan S, Zhao E, Kryczek I, et al. Tumor-associated macrophages produce interleukin 6 and signal via STAT3 to promote expansion of human hepatocellular carcinoma stem cells. *Gastroenterology* 2014;147:1393–404.
- MacParland SA, Liu JC, Ma X-Z, et al. Single cell RNA sequencing of human liver reveals distinct intrahepatic macrophage populations. *Nat Commun* 2018;9:4383.
- Ramachandran P, Dobie R, Wilson-Kanamori JR, et al. Resolving the fibrotic niche of human liver cirrhosis at single-cell level. *Nature* 2019;575:512–8.
- Xiong X, Kuang H, Ansari S, et al. Landscape of intercellular crosstalk in healthy and NASH liver revealed by single-cell secretome gene analysis. *Mol Cell* 2019;75:644–60.
- Wilson CL, Jurk D, Fullard N, et al. NFκB1 is a suppressor of neutrophil-driven hepatocellular carcinoma. *Nat Commun* 2015;6:6818.
- Wu J, Li J, Salcedo R, et al. The proinflammatory myeloid cell receptor TREM-1 controls Kupffer cell activation and development of hepatocellular carcinoma. *Cancer Res* 2012;72:3977–86.
- Cardin R, Piciocchi M, Bortolami M, et al. Oxidative damage in the progression of chronic liver disease to hepatocellular carcinoma: an intricate pathway. *World J Gastroenterol* 2014;20:3078–86.
- Paula Santos N, Colaço A, Gil da Costa RM, et al. N-Diethylnitrosamine mouse hepatotoxicity: time-related effects on histology and oxidative stress. *Exp Toxicol Pathol* 2014;66:429–36.
- Wang H, Sun L, Su L, et al. Mixed lineage kinase domain-like protein MLKL causes necrotic membrane disruption upon phosphorylation by RIP3. *Mol Cell* 2014;54:133–46.
- Hernandez-Gea V, Toffanin S, Friedman SL, et al. Role of the microenvironment in the pathogenesis and treatment of hepatocellular carcinoma. *Gastroenterology* 2013;144:512–27.
- Murray PJ. Macrophage polarization. *Annu Rev Physiol* 2017;79:541–66.
- Li H, You H, Fan X, et al. Hepatic macrophages in liver fibrosis: pathogenesis and potential therapeutic targets. *BMJ Open Gastroenterol* 2016;3:e000079.
- Brown ZI, Heinrich B, Gretchen TF. Mouse models of hepatocellular carcinoma: an overview and highlights for immunotherapy research. *Nat Rev Gastroenterol Hepatol* 2018;15:536–54.
- Filliol A, Schwabe RF. Contributions of fibroblasts, extracellular matrix, stiffness, and mechanosensing to hepatocarcinogenesis. *Semin Liver Dis* 2019;39:315–33.
- Grohmann M, Wiede F, Dodd GT, et al. Obesity drives STAT-1-dependent NASH and STAT-3-Dependent HCC. *Cell* 2018;175:1289–306. e20.
- Shi J-H, Line P-D. Effect of liver regeneration on malignant hepatic tumors. *World J Gastroenterol* 2014;20:16167–77.
- Mohammed FF, Khokha R. Thinking outside the cell: proteases regulate hepatocyte division. *Trends Cell Biol* 2005;15:555–63.
- Cressman DE, Greenbaum LE, DeAngelis RA, et al. Liver failure and defective hepatocyte regeneration in interleukin-6-deficient mice. *Science* 1996;274:1379–83.
- Della Fazio MA, Servillo G. Foie GRAS and liver regeneration: a fat dilemma. *Cell Stress* 2018;2:162–75.
- Rudnick DA, Davidson NO. Functional relationships between lipid metabolism and liver regeneration. *Int J Hepatol* 2012;2012:1–8.
- Thompson AI, Conroy KP, Henderson NC. Hepatic stellate cells: central modulators of hepatic carcinogenesis. *BMC Gastroenterol* 2015;15:63.
- Kocabayoglu P, Friedman SL. Cellular basis of hepatic fibrosis and its role in inflammation and cancer. *Front Biosci* 2013;5:217–30.
- Yang JD, Nakamura I, Roberts LR. The tumor microenvironment in hepatocellular carcinoma: current status and therapeutic targets. *Semin Cancer Biol* 2011;21:35–43.
- Khawar IA, Park JK, Jung ES, et al. Three dimensional Mixed-Cell spheroids mimic Stroma-Mediated chemoresistance and invasive migration in hepatocellular carcinoma. *Neoplasia* 2018;20:800–12.
- Jung H-R, Kang HM, Ryu J-W, et al. Cell spheroids with enhanced aggressiveness to mimic human liver cancer in vitro and in vivo. *Sci Rep* 2017;7:10499.
- Perugorria MJ, Olaizola P, Labiano I, et al. Wnt-β-catenin signalling in liver development, health and disease. *Nat Rev Gastroenterol Hepatol* 2019;16:121–36.
- Russell JO, Monga SP. Wnt/β-Catenin Signaling in Liver Development, Homeostasis, and Pathobiology. *Annu Rev Pathol* 2018;13:351–78.
- Otero K, Shinohara M, Zhao H, et al. Trem2 and β-catenin regulate bone homeostasis by controlling the rate of osteoclastogenesis. *J Immunol* 2012;188:2612–21.
- Zheng H, Jia L, Liu C-C, et al. Trem2 promotes microglial survival by activating Wnt/β-catenin pathway. *J Neurosci* 2017;37:1772–84.
- Yao Y, Li H, Chen J, et al. Trem-2 serves as a negative immune regulator through Syk pathway in an IL-10 dependent manner in lung cancer. *Oncotarget* 2016;7:29620–34.
- Tang W, Lv B, Yang B, et al. Trem2 acts as a tumor suppressor in hepatocellular carcinoma by targeting the PI3K/Akt/β-catenin pathway. *Oncogenesis* 2019;8:9.
- Barash H, R Gross E, Edrei Y, et al. Accelerated carcinogenesis following liver regeneration is associated with chronic inflammation-induced double-strand DNA breaks. *Proc Natl Acad Sci U S A* 2010;107:2207–12.
- Li H, Zhang L. Liver regeneration microenvironment of hepatocellular carcinoma for prevention and therapy. *Oncotarget* 2017;8:1805–13.



- 59 Campbell JS, Riehle KJ, Brooling JT, *et al.* Proinflammatory cytokine production in liver regeneration is MyD88-dependent, but independent of CD14, TLR2, and TLR4. *J Immunol* 2006;176:2522–8.
- 60 Seki E, Tsutsui H, Iimuro Y, *et al.* Contribution of Toll-like receptor/myeloid differentiation factor 88 signaling to murine liver regeneration. *Hepatology* 2005;41:443–50.
- 61 Sharif O, Gawish R, Warszawska JM, *et al.* The triggering receptor expressed on myeloid cells 2 inhibits complement component 1q effector mechanisms and exerts detrimental effects during pneumococcal pneumonia. *PLoS Pathog* 2014;10:e1004167.
- 62 Pei W, Tanaka K, Huang SC, *et al.* Extracellular HSP60 triggers tissue regeneration and wound healing by regulating inflammation and cell proliferation. *NPJ Regen Med* 2016;1:16013.
- 63 Otsu K, Kato S, Ohtake K, *et al.* Alteration of rat liver proteoglycans during regeneration. *Arch Biochem Biophys* 1992;294:544–9.
- 64 Gomez Perdiguero E, Klapproth K, Schulz C, *et al.* Tissue-resident macrophages originate from yolk-sac-derived erythro-myeloid progenitors. *Nature* 2015;518:547–51.
- 65 Zigmund E, Samia-Grinberg S, Pasmanik-Chor M, *et al.* Infiltrating monocyte-derived macrophages and resident Kupffer cells display different ontogeny and functions in acute liver injury. *J Immunol* 2014;193:344–53.
- 66 Amann T, Bataille F, Spruss T, *et al.* Activated hepatic stellate cells promote tumorigenicity of hepatocellular carcinoma. *Cancer Sci* 2009;100:646–53.
- 67 Funato Y, Michiue T, Asashima M, *et al.* The thioredoxin-related redox-regulating protein nucleoredoxin inhibits Wnt-beta-catenin signalling through dishevelled. *Nat Cell Biol* 2006;8:501–8.
- 68 Nathan C, Cunningham-Bussell A. Beyond oxidative stress: an Immunologist's guide to reactive oxygen species. *Nat Rev Immunol* 2013;13:349–61.
- 69 Kosack L, Gawish R, Lercher A, *et al.* The lipid-sensor TREM2 aggravates disease in a model of LCMV-induced hepatitis. *Sci Rep* 2017;7:11289.
- 70 Stracquadanio G, Wang X, Wallace MD, *et al.* The importance of p53 pathway genetics in inherited and somatic cancer genomes. *Nat Rev Cancer* 2016;16:251–65.